UNIVERSITY OF TARTU

Faculty of Science and Technology

Institute of Chemistry

Martinš Jansons

CHARACTERIZATION OF NATURAL SEDIMENTARY DOLOMITE AND LIMESTONE REFERENCE MATERIALS FROM GEOLOGICAL SURVEY OF ESTONIA USING LA-ICP-MS

Master's Thesis

(30 ECTS in Applied Measurement Science)

Supervisors:

Päärn Paiste

Kalle Kirsimäe

Department of Geology

Institute of Ecology And Earth Sciences

Tartu University

Tartu – 2016

Looduslike Eesti Geoloogiateenistuse lubjakivi ja dolomiidi referentsmaterjalide mikroanalüüs kasutades LA-ICP-MS'i

Eesti Geoloogiateenistuse poolt looduslike settekivimite baasil valmistatud dolomiidi (Es-16, Es-18) ja lubjakivi (Es-3, Es-14, Es-17) referentsmaterjale on röntgenfluoresentsanalüüsi kalibratisoonistandarditena kasutatud mitmetes Eesti laborites. Käesolevas töös on kasutatud nende materjalide homogeensuse testimiseks ja mikrokarakteriseerimiseks laserablatsiooniga induktiivsidestatud plasma mass-spektromeetriat. Analüüsides kasutati kalibreerimiseks MACS-3 ja NIST 612 referentsmaterjale ja võrdluseks analüüsiti CRPG CAL-S loodusliku lubjakivi standardit. Es-standardite sobivust mikroanalüütiliste referentsmaterjalidena hinnati homogeensuse indeksi ja proovi heterogeensusest põhjustatud määramatuse alusel. Tulemuste alusel olid kõige homogeensemad Es-17 ja Es-16 standardid. Es-17, Es-3 ja Es-16 standardites olid Cs ja Rb homogeensema jaotuse ja kõrgema kontsentratsiooniga kui MACS-3 standardis. Haruldaste muldmetallide heterogeenset jaotumist täheldati standardites Es-14, Es-18 ja Es-17.

Märksõnad: *LA-ICP-MS, homegeensus, kaltsiumkarbonaat, referentsmaterjalid,*

Characterization of natural sedimentary dolomite and limestone reference materials from Geological Survey of Estonia using LA-ICP-MS

Sedimentary dolomite (Es-16, Es-18) and limestone (Es-3, Es-14, Es-17) from Geological Survey of Estonia have been used as reference materials in X-ray fluorescence analysis in Estonian laboratories. Homogeneity of these materials was investigated with laser-ablation inductively coupled plasma mass-spectrometry using MACS-3 and NIST612 certified reference materials for calibration. Natural limestone CAL-S from CRPG was analyzed for overall comparison. Potential application of Es's as micro-analytical reference materials was evaluated by quantification of uncertainty due to inhomogeneity and estimation of homogeneity index. Es-17 and Es-16 were found most homogenous. More homogenous distribution and higher concentrations of Cs and Rb were found in Es-17, Es-3 and Es-16 than in MACS-3. Inhomogenous distribution of rare earth elements was observed in Es-14, Es-18 and Es-17.

Keywords: *LA-ICP-MS, homogeneity, calcium carbonate, reference materials,*

CERCS code: P300 Analytical chemistry

ABBREVIATIONS

AAS	atomic absorption spectroscopy
AES	atomic emission spectroscopy
AFM	atomic force microscopy
ANOVA	analysis of variance
CRM	certified reference material
CRPG	*Centre de Recherches Pétrographiques et Géochimiques*
DCP-AES	direct current plasma atomic emission spectrometry
EPMA	electron probe micro-analysis
IAG	International Association of Geoanalysts
ICP	inductively coupled plasma
ICP-MS	inductively coupled plasma mass spectrometry
ICP-OES	inductively coupled plasma optical emission spectrometry
INAA	instrumental neutron activation analysis
LA	laser ablation
LA-ICP-MS	laser ablation inductively coupled plasma mass spectrometry
LIBS	laser-induced breakdown spectroscopy
LMD-ICP-MS	laser micro-dissection inductively coupled plasma mass spectrometry
LOD	limit of detection
LOQ	limit of quantification
MS	mean square
NF-LA-ICP-MS	near-field laser ablation inductively coupled plasma mass spectrometry
NIST	National Institute of Standards and Technology
REE	rare earth element
RM	reference material
RSD	relative standard deviation
SI	*Système international d'unités*
SIMS	secondary ion mass spectrometry
USGS	United States Geological Survey
XRF	X-ray fluorescence

TABLE OF CONTENTS

1. INTRODUCTION

While liquid based inductively coupled plasma mass spectrometry (ICP-MS) is an established analytical method with possibility to detect different isotopes of elements, low detection limits, capability to analyze many elements simultaneously, wide dynamic range and high throughput, then laser ablation (LA) is a developing method of sample introduction that offers spatial micro-analysis with resolution down to several micrometers and rapid introduction of below microgram level test portions of samples without the usual time consuming digestion procedures done for liquid sample introduction. Geochemical laboratories were early adopters of LA-ICP-MS, and it has established applications in geochronology, analysis of trace element concentrations in geological samples as well as applications in environmental research, material science, archeology and forensics [1], [2].

The weak point of LA-ICP-MS analysis is the calibration and different matrix effects. Inductively coupled plasma (ICP) ionization typically requires matrix matched calibration, and even with matrix matched calibration interferences hinder analysis of many isotopes. If requirement for limit of quantification (LOQ) is sufficiently low, interference occurs for almost every isotope. In addition to the matrix effects arising in ICP, sample introduction by LA adds possibility for more matrix effects, mainly because of the complex interaction of laser beam with the sample. Also, matrix matched reference materials (RM's) may be unavailable or difficult to prepare. This is an especially acute problem when carbonate RM's are concerned as there is only one matrix matched CRM available on the market [3].

LA-ICP-MS is increasingly used for spatial micro-analysis of trace elements in carbonate materials such as speleothems, shells, corals, otoliths and carbonate rocks. Jochum et al. (2011) have characterized the spectral interferences that can occur in analysis of speleothems and biogenic carbonate materials and the NIST 612 glass RM, which is often used for calibration in LA-ICP-MS procedures [4].

In this thesis three sedimentary dolomite (Es-4, Es-16, Es-18) and three sedimentary limestone (Es-3, Es-14, Es-17) candidate RM's provided by the Geological Survey of Estonia are undertaken for characterization and microanalysis by LA-ICP-MS. Element concentrations and the respective expanded uncertainties are estimated. Homogeneity of elements in the RM's is estimated in order to evaluate the potential application of these materials as micro-analytical natural carbonate RM's.

2. LITERATURE OVERVIEW

2.1. Principles of LA-ICP-MS operation

LA-ICP-MS has become a widely adopted multi-element micro-analytical technique. It operates by directing a pulsed laser beam shaped by an aperture through the optical components to the sample in order to evaporate it at chosen location from the surface. For round apertures diameters of the resulting spot range from 5 to 200 μm. The sample holder can be moved in all directions to ensure spot selection and line or raster scan modes of ablation. Vertical direction enables focusing [1], [5], [6].

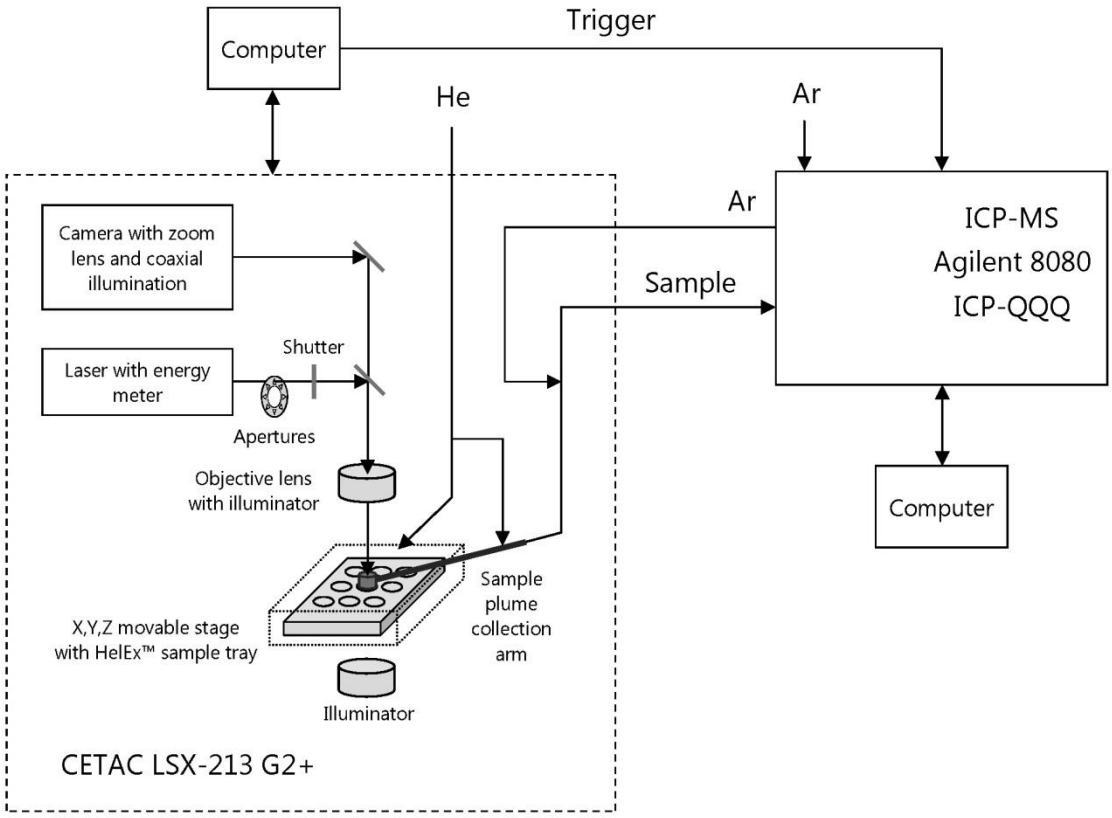

Figure 2.1.1. Simplified schematic of LA-ICP-MS setup used in the present thesis.

Each laser pulse generates a transient micro-plasma immediately above the ablation spot. Ablated sample aerosol is directed by helium gas flow from the hermetically sealed sample holder to ICP-MS system, which records the transient signal. Variation in aerosol amount, particle size distribution and composition may occur not only during ablation, but also during transport, which contributes to elemental fractionation. Elemental fractionation is the difference in signal between the first part and the second part of the transient ablation signal. Attention should be paid to possible spectral interferences and matrix matching of samples

with calibrants [5], [7]. The parameters to be optimized in LA are laser beam wavelength, pulse duration, repetition rate and fluence (radiant exposure) [8]. Depending on the experiment, fluence ranges from a few to few tens of $J \cdot cm^{-2}$ [8], [9].

With improving laser ablation technology, the wavelength of laser beam has reduced over time from IR to UV wavelengths, which show better repeatability and slightly decreased elemental fractionation. This has been attributed to a different particle size distribution of generated sample aerosol at different wavelengths [10]. Also, absorption by sample at the wavelength of choice should be considered [11].

LA systems can be classified according to the laser pulse duration into nanosecond and femtosecond systems. In nanosecond systems the wavelength is the main factor determining ablation quality. Femtosecond laser systems ablate materials with different physical and chemical properties in a similar way, which is attributed to the short interaction time of laser pulse with the sample and insufficient time given for the material to melt. The minimized fractionation results in ablated particles that are more representative of the sample [8]. The main mechanisms suggested for material removal are Coulomb explosion and thermal vaporization. Due to the short pulse duration in femtosecond laser systems, Coulomb explosion is the main mechanism and material is removed with minimal thermal effects taking place, which results in sharp-edged, well-defined ablation craters [9]. Choice of wavelength using femtosecond LA systems depends on the material to be analyzed, particularly whether it is dielectric or conducting, because for dielectric targets a part of the laser pulse energy is spent on promotion of electrons from valence to conduction band, after which ablation mechanism is similar in dielectrics and conductors [12].

Apart from particles ejected from the ablation site, optical emission could also be analyzed, which is the basis of LIBS spectroscopy [9].

2.2. Applications of LA-ICP-MS

It is well known that the majority of applications using ICP are environmental, geochemical, biomedical or semiconductor related [13], [14]. Environmental laboratories are one of the major users of ICP instruments in part due to the need to perform routine analysis of trace elements in drinking water, for example, according to the European Union directive (98/83/EC) requirements [15]. Recently, many of these laboratories have been phasing out of use other elemental analysis methods in favor of ICP-MS [16]. While LA sampling is not

used for routine environmental applications, occasionally it is used in environmental research [17].

Since sampling of water at selected spots from nature often involves a risk of non-representativeness, effort has been invested in development of passive sampling devices, which require calibration at controlled conditions, but decrease chance of missing short-term pollution events and allow estimation of time weighted average concentrations of pollutants. In one study regarding passive samplers, the chelating disc was successfully analyzed using LA-ICP-MS. This allowed to skip elution of the sampler and decrease risk of contamination during handling, but, most importantly, the "dry plasma" produced during LA reduced oxide interferences [18], [19].

Research utilizing the micrometer level spatial resolution of LA-ICP-MS include raster imaging of trace elements in biological tissues [20], mostly line scan, but raster imaging has been used as well in analysis of fish otoliths [21], speleothems [4], shells [22], corals [23], rocks [24], food and plants [25], [26], annual growth rings of trees [27], hair [28] and samples analyzed as forensic evidence, such as glass, paint coatings, ink on paper, fibers, cannabis, gemstones, bricks, gold and silver objects [29].

Recent research on the distribution of trace elements in biological tissues, such as brain, also called bioimaging of elements, has been of interest because of the important role of metal homeostasis in brain functions and occurrence and treatment of brain diseases. The advantage of LA-ICP-MS in this case is the high sensitivity and possibility to analyze different isotopes [30]. Conventional LA sampling setups enable spatial resolution down to 10 μm, however, in order to study single cells and subcellular structures, special nano-LA-ICP-MS setups, such as near-field LA-ICP-MS and laser micro-dissection ICP-MS are being developed. Laser microdissection ICP-MS (LMD-ICP-MS) setups can achieve resolution around 1 μm, but developers of NF-LA-ICP-MS are expecting to reach resolution down to 50 nm, using a thin silver needle as the focusing element under defocused laser beam and targeting controlled electronically as in AFM [30], [31].

Elemental bioimaging has been applied to food as well. In order to study the element distribution in rice seeds, which tend to accumulate trace As, Sb and Cd, conventional LA-ICP-MS was applied. The samples were analyzed in spot ablation mode with spot diameter of 50 μm, repetition rate of 20 Hz and fluence range 12.2…18.7 $J \cdot cm^{-2}$, and the spots were arranged in grids over the samples [25].

Analysis of otoliths has become an established research application for LA-ICP-MS. Otoliths are composed mainly of calcium carbonate in the form of aragonite with minor

organic matrix. Mineralization of otoliths occurs during the life of fish. Elements from ambient water get incorporated into the otoliths, and therefore spatial analysis of otoliths reveals environmental conditions experienced by the fish during its life. However, it has been shown that otoliths can contain vaterite inclusions, which exhibit different composition for some elements in comparison to aragonite. The analysis of both polymorphs in a single replicate could result in misinterpretation of the environmental history [32]. For analysis of larval otoliths beam diameter of 5…11 μm and low energy (2.7 $J \cdot cm^{-2}$) should be used and raster scanning mode has been suggested to circumvent difficulty in achieving precise alignment of laser beam and camera center point [21].

Analysis of Hg, Cu and Zn concentration along grizzly bear hair has been suggested as good indicators of salmon consumption. This is useful for estimation of trace metal exposure and could possibly be applied to other mammals as well as a non-invasive tool for monitoring programs [28].

While chemical analysis of the composition of tree annual growth rings has been successfully used to study past events of pollution and single large volcanic events, it was hypothesized that LA-ICP-MS analysis of tree annual growth rings could reveal persistent fluctuating volcanic activity as well. However, it was concluded that due to lack of reproducibility among samples and high variability of results around the trunk, chemical composition of annual growth rings does not provide useful data for that purpose [27].

Analysis of forensic evidence is important because it allows linking the suspect to physical evidence recovered from the crime scene to ensure a successful prosecution. The most prominent applications are analysis of glass fragments, paint, including layered paint samples, ink and paper. The advantage of LA-ICP-MS in this case is spatial resolution and low LOD's. Spatial resolution along the ablation depth axis is advantageous when compared to XRF because of the deep penetration of X-rays, which complicates analysis of layered paint samples. Also, excitation volume varies depending on element. Goal of forensic analysis most often is to discriminate between different samples or confirm the common origin of two samples, chemometric methods for processing results therefore are used, such as ANOVA, discriminant analysis, cluster analysis, principal component analysis. This way variables that offer the most reliable discrimination are determined [29].

LA-ICP-MS was applied for analysis of individual solid, liquid, gas or mixed phase inclusions in minerals. A recent development is isotope ratio analysis of individual fluid inclusions by multicollector ICP-MS, e.g., Pb and Sr isotope ratios. The advantage of LA-ICP-MS here is that a volume is always analyzed and the entire inclusion content can be

analyzed, which is important, because the sample amount is already limited by size of inclusion. Best transient signal is obtained if spot diameter is selected such that maximum amount of inclusion is analyzed with respect to the host mineral, thus minimizing LOD's. Depending on the character of transient signal of elements in host and inclusion, selection of signal intervals corresponding to background, host mineral and inclusion is done and are used for quantification. Internal overpressure of inclusions may result in spikes and shorter signals after release, as well as loss of analytes due to redeposition on sample surface. Internal standardization is necessary for analysis of fluid inclusions to correct for ablation yield, especially in case if inclusion contents erupt upon opening. External calibration has proved impossible, because the absolute signal intensities are not related to element concentrations [5], [33].

2.3. Calibration of LA-ICP-MS

Full quantitative analysis with linear regression linking concentration with signal intensity requires separate RM's with content of analytes at different concentration levels within required range. Such RM's are usually not available and if possible can be prepared in-house. An example of such a procedure has been demonstrated by analysis of Mn, Co, Ni, Cu, Cd and Pb in form of inorganic salts homogenized with a matrix of active pharmaceutical powder and pressed into pellets showing R^2 better than 0.997, and the repeatability RSD's below 10 % [34].

Using a specialized sample introduction accessory with a desolvating nebulizer, it is possible to carry out standard additions. No solid RM's would be needed and it would then be required only to know the approximate expected count rates for analytes in sample to determine the amount of standard to be added online [35] This method is, however, not applicable to most types of analysis using LA-ICP-MS and is not widely used.

The most common calibration approach is external calibration with normalization to a naturally occurring internal standard as shown in equation 2.3.1-2.3.2. The concentration of internal standard is determined beforehand using an alternative method [36].

Count rate at a particular mass-to-charge ratio is usually meaningless, therefore mean background subtracted count rates normalized to internal standard should be used to correct for ablated amount of sample. It is assumed that the isotopic fingerprint is the same in samples and calibrants.

$$C_{AN_{SAM}} = \frac{R_{AN_{SAM}}}{S} \tag{2.3.1}$$

$$C_{AN_{SAM}} = C_{AN_{CAL}} \frac{R_{AN_{SAM}}}{R_{AN_{CAL}}} \left(\frac{C_{IS_{SAM}}}{R_{IS_{SAM}}} \frac{R_{IS_{CAL}}}{C_{IS_{CAL}}} \right) \tag{2.3.2}$$

$$C_{AN_{SAM}} = \frac{R_{AN_{SAM}}}{R_{IS_{SAM}}} \cdot C_{IS_{SAM}} \cdot \left(\frac{C_{AN_{CAL}}}{R_{AN_{CAL}}} \frac{R_{IS_{CAL}}}{C_{IS_{CAL}}} \right)_{interpolated} \tag{2.3.3}$$

where S – sensitivity, cps/ppm;

$C_{AN_{SAM}}$ – concentration of analyte in sample, ppm;

$C_{IS_{SAM}}$ – concentration of internal standard in sample, ppm;

$R_{AN_{SAM}}$ – count rate of analyte in sample, cps;

$R_{IS_{SAM}}$ – count rate of internal standard in sample, cps;

$C_{AN_{CAL}}$ – concentration of analyte in calibrant, ppm;

$C_{IS_{CAL}}$ – concentration of internal standard in calibrant, ppm;

$R_{AN_{CAL}}$ – count rate of analyte in calibrant, cps;

$R_{IS_{CAL}}$ – count rate of internal standard in calibrant, cps.

Equation 2.3.2 can be rearranged to give equation 2.3.3, where the interpolated term is determined from several analyses of RM's in order to correct for changes in sensitivity over time. If there was no drift, the interpolated term would be constant, however, in ICP-MS this is rarely the case. Therefore the samples should be analyzed between analyses of RM's. The transient signals should be reviewed manually for discrepancies and a faulty RM analysis removed. If more than one repeated measurement in a row is carried out on the RM, the sequential measurements can be averaged in order to prevent a single faulty analysis distorting the interpolation.

When using external calibration with normalization to a naturally occurring internal standard, the ablation conditions would preferably be kept the same for analyses of samples and calibrants [11]. Some authors have chosen different conditions. For example, for element bioimaging in food, line scan mode at spot diameter of 50 μm, scan rate of 50 μm·s^{-1} and repetition rate of 10 Hz was used for ablation of calibrants, which is different from the single spot ablation conditions applied to samples [25]. Matrix matched calibration and keeping ablation conditions the same for analysis of calibrants and samples is recommended. If different ablation conditions are used, element fractionation may be different in both analyses, which would result in poorer accuracy of the results [11].

Choice of different ablation conditions for samples and calibrants may lead to a greater influence on the results by mass load induced matrix effects. Significant mass load induced matrix effects have been reported for chalcophile/siderophile elements, e.g., Zn, Cu and Pb, where matrix composition, spot diameter and laser wavelength are the main influencing factors. The discrepancy in sensitivity increases with increasing ablation spot diameter and is different in different matrices. This has been attributed to the elemental fractionation factors being unequal to one [10].

Comparison of LA-ICP-MS measurements with solution ICP-MS measurements is often used to assure quality of the measurement procedure, which includes calibration. The number of measurements performed on the sample by LA-ICP-MS in spot ablation mode is critical, because the average must be compared to the solution ICP-MS measurement [28]. Whether or not the LA-ICP-MS and solution ICP-MS data match, depends on how homogeneously the element of interest is distributed in the material. Even if trueness suffers from chosen calibration approach, LA-ICP-MS is still useful to determine the distribution of elements in sample [1].

2.4. Reference materials

In measurement science in general the CRM's are preferred over other classes of RM's. This is so because the certifying body orchestrates measurements by methods that yield values with uncertainties that are appropriate to the expected end-use of the CRM by involving laboratories of high scientific status and quality, thus the CRM produced will have a sufficiently accurate property value with a suitable uncertainty, the CRM values will likely be located close to the realization of SI system unit in the traceability chain, and as required the stability and homogeneity of the CRM will be characterized sufficiently well. The RM's could be certified using measurements by a single definitive method in a single laboratory, where a definitive method is a method that has a valid and well-described theoretical foundation and the results have negligible systematic errors relative to end-use requirements, or by measurements from interlaboratory testing, where in the interlaboratory testing, preferably, at least 15 laboratories of equal capability in determination of the characteristics are involved, or by formulation, where weighing and/or volumetric data are used [37], [38].

As recommended by ISO Guide 35:1989, any CRM must be sufficiently homogenous that the property value measured on one portion of the batch applies to any other portion of the batch within acceptable limits of uncertainty. In many cases precision of a method is

affected by test portion size, therefore homogeneity of an RM is defined for a given test portion size. If the material is not homogenous enough with respect to the property value, it cannot be certified. If an acceptable degree of inhomogeneity can be detected, the combined certified uncertainty must include uncertainty due to inhomogeneity. If trends in inhomogeneity are detected, they must be described mathematically in order to certify the RM. If there is significant inhomogeneity between units, each unit may need to be certified separately [37], [39].

To date, more than 300 bulk RM's for geochemical analysis have been developed by a number of agencies world-wide. The demand has been exceeding supply and is expected to do so in the future [38]. Due to the nature of micro-analysis, homogeneity is a critical aspect for micro-analytical RM's. Minimum homogenous test portion must be determined and the potential differences between sampling volumes during a typical micro-analysis must be determined. The choice of RM's suitable for LA-ICP-MS is limited and depends on application, for example, float glass RM's available for forensic analysis of glass [29], synthetic glass RM's from NIST SRM 610-617 series widely used for different applications [6], synthetic basaltic glass RM's USGS GSA-1G, GSC-1G, GSD-1G, GSE-1G and basalt glass USGS BCR-2G [40], synthetic sulfide RM's USGS MASS-1 and MASS-3 [1], [41]. Some other micro-analytical RM's are currently being developed by USGS, such as synthetic calcium phosphate and synthetic sulfide [41].

NIST glasses are made of high purity quartz sand, alumina, soda ash and calcium carbonate, which were fused in a Pt/Rh lined electrically heated furnace. About 100 kg of NIST SRM 610-611, 612-613, 614-615 and 616-617 were prepared by doping with sixty one trace elements to nominal concentrations of 500, 50, 1 and 0.02 $\mu g \cdot g^{-1}$. Each glass is available as 3 mm (NIST SRM 610, 612, 614, 616) or 1 mm (NIST SRM 611, 613, 615, 617) wafers, hence the eight reference glasses have only four glass compositions.

For purposes of calibration of LA-ICP-MS and other micro-analytical techniques, NIST reference materials of the SRM series (610-617) are used most frequently.

NIST SRM 610-611 and 612-613 have the advantage that they contain many trace elements, whose concentrations are uniform and sufficiently high for a precise primary calibration (around 400 $\mu g \cdot g^{-1}$ for SRM 610-611, around 40 $\mu g \cdot g^{-1}$ for SRM 612-613).

The disadvantages are that the NIST glasses, with the exception of a few elements, have not been certified and were not designed for micro-analytical purposes. Because of this, several authors, Pearce et al. (1997), Rocholl et al. (1997), compiled published data to derive consensus values [6].

The NIST 610 and 612 glasses used for calibration have only been certified for eight elements and not for micro-analytical purposes. Compilation values by Pearce et al. (1997), which were commonly used for data quantification, were based on analyses that are more than 15 years old and do not comply with the guidelines of the International Organization for Standardization (ISO) for certification of reference materials. For analysis of, for example, calcium carbonate matrices, the calcium carbonate matrix is quite different from NIST glass silicate matrix. It is well known that the accuracy of LA-ICP-MS analyses is affected by matrix effects [4], [6].

The interest in the chemical information recorded in carbonates is increasing for environmental and climate studies. Use of LA-ICP-MS has been increasing in quantification of trace elements in materials, such as shells, corals, otoliths and speleothems, however, because of the lack of carbonate reference materials, NIST 610 and 612 were commonly used for calibration. USGS attempted to solve this problem by developing MACS-3 synthetic carbonate RM primarily for the marine community. MACS-3 was prepared using a co-precipitation process. However, MACS-3 has not been certified yet for any of the 62 elements. Preliminary certificate with values based on USGS bulk analysis methods is available [4], [42].

2.5. Matrix effects in analysis of NIST 612 and calcium carbonate matrices

Matrix effects due to ablation process, ICP and effects due to interferences, which occur if there is a matrix mismatch, determine the LOQ of each analyte. It is essential to know how the matrix effects would affect each analyte in order to be able to derive conclusions about the trueness of measurement results.

Interferences encountered in analysis of NIST 612 and calcium carbonate matrix (natural stalagmite) were characterized by Jochum et al. (2012) using sector field ICP-MS (at $m/\Delta m \approx 4000$) [4]. Interference free isotopes were determined. Resolved interferences in silicate NIST 612 and calcium carbonate material were estimated, assigned and tabulated according to severity of interference. The resolution necessary for resolving different isotopes was given [4].

Most of interferences cannot be corrected by a gas blank, unless the isotope is affected mainly by interferences originating from plasma and to a sufficiently low degree. Interferences originating from the carbonate matrix can overlap several isotopes by more than 10 %. These isotopes were $^{24}Mg^+$, $^{29}Si^+$, $^{30}Si^+$, $^{33}S^+$, $^{34}S^+$, $^{45}Sc^+$, $^{52}Cr^+$, $^{53}Cr^+$, $^{57}Fe^+$, $^{59}Co^+$ and

$^{60}Ni^{+}$. Interference free isotopes should be selected or higher resolution mass spectrometry used for analysis. In order to have acceptable trueness for trace elements affected by interferences originating from other trace elements, it is important that the concentrations of both are around the same order of magnitude. Such isotopes are $^{45}Sc^{+}$, $^{63}Cu^{+}$, $^{67}Zn^{+}$, $^{68}Zn^{+}$, $^{69}Ga^{+}$, $^{151}Eu^{+}$, $^{153}Eu^{+}$, $^{155}Gd^{+}$, $^{157}Gd^{+}$, $^{159}Tb^{+}$, $^{204}Pb^{+}$, which are affected by singly charged polyatomic interferences, and $^{69}Ga^{+}$, $^{71}Ga^{+}$, $^{72}Ge^{+}$, $^{73}Ge^{+}$, $^{75}As^{+}$, $^{77}Se^{+}$, $^{85}Rb^{+}$, $^{84}Sr^{+}$, $^{86}Sr^{+}$, $^{88}Sr^{+}$, $^{119}Sn^{+}$, which are affected by doubly charged interferences [4]. Therefore a ratio of the source of interference to the analyte being too large (e.g., >1000) in sample or calibrant would affect trueness. The permissible ratio is determined by the amount of interfering species formed. In case of polyatomic interference it could be estimated by equilibrium constants. In case of multiply charged interference it could be estimated by ionization potentials.

Element fractionation due to ablation process causes the relative sensitivity factors normalized to NIST 612 to be different from unity in natural carbonate, especially for Nd, La, W, Pb, Tl, Ni, Fe, Ga, Ge, Sn, Sb, Cu, An, Cd, while refractory lithophile elements and REE's are much less affected. The relative sensitivity factors are on average better with 193 nm laser system [4].

Significant mass load dependent matrix effects were described for Cu, Zn and Pb, thus the element to internal standard ratio varies across different test portion masses, which are varied by changing the spot diameter. Also the test portion masses are different for different laser wavelengths at same spot diameter [4].

Matrix matching is necessary for elements strongly affected by interferences and fractionation. Then the trueness could be acceptable provided that the interference does not exceed the signal from analyte itself by several orders of magnitude, which would make the changes in analyte signal undetectable.

2.6. Experimental determination of homogeneity of micro-analytical RM's

Micro-analysis has been proposed to experimentally determine the minimum test portion down to which CRM certificates remain valid on the basis that the uncertainty due to material inhomogeneity is inversely proportional to the square root of analyzed test portion mass. High precision is the main requirement for any method used for homogeneity testing, because this determines the ability to detect small differences between analyzed samples. Even if such a method is not acceptable for use in certification, because of lack of traceability, it would still be acceptable for homogeneity tests because of the high precision [43].

Therefore, LA-ICP-MS would be a suitable method for determining the homogeneity of trace elements due to the high spatial resolution and precision.

Almost all geological samples are inhomogenous if a small enough test portion is taken for analysis. The better is the precision of a measurement method, the higher degree of homogeneity is required. Produced RM's can be inhomogenous within units as well as between units, which is referred to as within-unit and between-unit homogeneity, and is especially true for powdered RM's. Inhomogeneity in RM's must be quantified and included in the uncertainty of the reference value. ANOVA can be used to determine if there is a difference between these types of inhomogeneity in a candidate RM that is considered homogenous.

Table 2.6.1. ANOVA table for two-stage nested design of an interlaboratory program, as suggested by ISO Guide 35:1989 [37].

Source	Sum of square	Degrees of freedom	Mean square	Expectation of mean square
Between laboratories	$SS_1 = qn\sum_{i=1}^{p}(\bar{x}_i - \bar{x})^2$	$f_1 = p - 1$	$MS_1 = \frac{SS_1}{f_1}$	$\sigma_W^2 + n\sigma_U^2 + qn\sigma_L^2$
Between units	$SS_2 = n\sum_{i=1}^{p}\sum_{j=1}^{q}\left(\bar{x}_{ij} - \bar{x}_i\right)^2$	$f_2 = p(q-1)$	$MS_2 = \frac{SS_2}{f_2}$	$\sigma_W^2 + n\sigma_U^2$
Measurement error	$SS_3 = \sum_{i=1}^{p}\sum_{j=1}^{q}\sum_{k=1}^{n}\left(x_{ijk} - \bar{x}_{ij}\right)^2$	$f_3 = pq(n-1)$	$MS_3 = \frac{SS_3}{f_3}$	σ_W^2

$$\sigma_L^2 \approx (MS_1 - MS_2)/qn \quad (2.6.1)$$

$$\sigma_U^2 \approx (MS_2 - MS_3)/n \quad (2.6.2)$$

$$\sigma_W^2 \approx MS_3 \quad (2.6.3)$$

where $\bar{x}$ – estimate of the grand mean;

x_{ijk} – the result *k* of sample unit *j* reported by laboratory *i*;

p – number of laboratories;

q – number of sample units per laboratory;

n – number of replicate determinations per sample unit;

$$F_{2|3} = MS_2/MS_3 \quad (2.6.4)$$

$$F_{1|2} = MS_1/MS_2 \quad (2.6.5)$$

Variance of the consensus value $\bar{x}$ is estimated as shown in equation 2.6.6 [37].

$$u^2 = \sqrt{MS_1/pqn} \quad (2.6.6)$$

The variance components depend on number of units from which samples are taken and the number of replicate measurements for each unit. For example, a two-stage nested design of an interlaboratory program, as suggested by ISO Guide 35:1989, to characterize the material and its homogeneity requires that each involved laboratory characterizes a number of repeated determinations for a number of sample units. ANOVA results from such a program are shown in table 2.6.1, where expected sources of variation and respective ANOVA results are listed. Mean squares from ANOVA can be used to estimate each contribution to combined uncertainty as shown in equations 2.6.1, 2.6.2 and 2.6.3. The F-ratio for statistical significance test for between-units (inhomogeneity) variance is shown in equation 2.6.4 and the F-ratio for between-laboratories variance is shown in equation 2.6.5. The respective degrees of freedom of mean squares determine the critical F-ratio to which the obtained F-ratio is compared [37], [38].

For purposes of a preliminary characterization of a single unit of a candidate RM ideally a similar ANOVA scheme could be applied, where the MS_3 would be expected to estimate instrumental precision from repeated measurement of the same volume from the same place in sample, MS_2 would be expected to estimate instrumental precision and inhomogeneity of a sample unit from measurements of volumes taken from different places in the sample, and finally MS_1 would be expected to estimate the latter and inhomogeneity between sample units, if more than one unit is analyzed. This scheme could also be modified to include the source of variation from measurements between laboratories as well if an interlaboratory program was intended.

Procedures used for homogeneity characterization usually employ replicate analysis to determine the analytical precision of the measurement, which affects the minimum level of inhomogeneity that can be detected. In LA-ICP-MS analysis the uncertainty components accounting for instrumental repeatability and inhomogeneity of material are difficult to separate, because the analyzed test portion is destroyed, thus truly repeated analysis of the same portion is not possible. Due to impossibility of measurement of the same volume from the same place in sample, because it is destroyed or altered during analysis, the mentioned ANOVA scheme could only be applied to micro-analysis using methods, such as EPMA, LA-ICP-MS and SIMS only after the analytical precision has been estimated [44].

Due to the fact that micro-analysis methods are destructive, it is difficult to distinguish between uncertainty due to measurement procedure $u_{meas.}$ (analytical precision) and

uncertainty due to material inhomogeneity $u_{inhom.}$ as shown in equation 2.6.7, because the experimentally determined uncertainty $u_{exp.}$ is always an overestimation of true inhomogeneity. Two possible approaches arise – the precision of procedure is estimated by some other means or determination of precision is carried out on a similar material of known homogeneity. Usually there is no such material available [39], [44].

$$u_{exp.}^2 = u_{meas.}^2 + u_{inhom.}^2 \tag{2.6.7}$$

Since the results in LA-ICP-MS are generated from counting of detector events, Poisson counting statistics can estimate a part of $u_{meas.}$, however, this will be limited to the detection step only, therefore $u_{meas.}$ consists of the uncertainty due to the procedure excluding detection $u_{proced.}$ and uncertainty $u_{Pois.}$ from counting process during detection, as shown in equation 2.6.8 [44].

$$u_{meas.}^2 = u_{proced.}^2 + u_{Pois.}^2 \tag{2.6.8}$$

For simplicity it could be assumed that uncertainty from counting process during detection step is the main contribution to measurement uncertainty as shown in equation 2.6.9 [44].

$$u_{meas.}^2 \approx u_{Pois.}^2 \tag{2.6.9}$$

For evaluation of homogeneity of micro-analytical RM's, the use of homogeneity index H has been suggested, which is a ratio of experimentally determined uncertainty and the estimate of measurement uncertainty, as shown in equation 2.6.10 [44].

$$H = \frac{E(u_{exp.})}{E(u_{meas.})} \approx \frac{s_{exp.}}{s_{rms.}} = \frac{s_{exp.}}{\sqrt{\frac{1}{N}\sum u_{Pois.i}^{\,2}}} \tag{2.6.10}$$

where E – expectation operator, because the true value is unknown;

$s_{exp.}$ – standard deviation of measurements of volumes taken from different places in the sample;

N – number of measurements;

$s_{rms.}$ – root mean square of estimated measurement uncertainties $u_{Pois.i}$.

For an ideally homogenous material with $u_{inhom.} = 0$ analyzed using a procedure where equation 2.6.9 holds true, the homogeneity index calculated would be $H = 1$. Homogeneity index of 1.5 has been observed for many solution ICP-MS analyses, indicating that the analytical precision is dominated by Poisson counting statistics [45]. Arbitrarily

selected criterion of $H < 3$ for confirming no detectable homogeneity has been used in some studies [46]–[48]. Due to the intrinsic uncertainty in experimental standard deviation and the estimated measurement uncertainties, the homogeneity index itself has an uncertainty, which decreases with increased number of measurements. Since homogeneity index is equal to the square root of a ratio of variances where both variances follow the *F*-distribution, critical values of homogeneity index were given for hypothesis testing at significance level α=0.05. The higher is the number of measurements, the lower is the critical homogeneity index and the lower is the contribution of inhomogeneity to the experimentally determined uncertainty that can be confirmed or rejected [44].

In order to include the uncertainty due to inhomogeneity in the certified combined uncertainty it must be quantified. If measurement uncertainty is known, then the uncertainty due to inhomogeneity can be calculated as shown in equation 2.6.11.

$$u_{inhom.} = \sqrt{u_{exp.}^2 - u_{meas.}^2} \qquad (2.6.11)$$

3. MATERIALS AND METHODS

3.1. Natural sedimentary dolomite and limestone RM's from Geological Survey of Estonia

This thesis concerns three sedimentary dolomite (Es-4, Es-16, Es-18) and three sedimentary limestone (Es-3, Es-14, Es-17) RM's from the Geological Survey of Estonia [49]. Es-4 (fine crystalline gray dolomite of Lower Silurian age, sampled in dolostones of Raikküla Stage in Mündi quarry, central Estonia), Es-16 (iron rich dolomite of Ordovician age, sampled in dolomitized limestones of Kunda Stage in Maardu quarry, northern Estonia), Es-18 (Silurian dolomite, sampled in secondary dolostones of Jaagarahu Stage in Anelema quarry, southwestern Estonia), Es-3 (organogenic gray limestone of Ordovician age, sampled from 2.0…2.4 m below the upper boundary of the Väo Formation in old Lasnamäe quarry), Es-14 (micritic yellowish-white limestone of Silurian age, sampled in Raikküla Stage limestones in depth interval 319.0…319.6 m of Taagepera core, southern Estonia) and Es-17 (argillaceous limestone of Silurian age, sampled Adavere Stage limestones in Valgu drillcore, northwestern Estonia). These RM's contain a wide range of elements with higher concentrations than in common sedimentary rocks [49].

The RM's Es-3 and Es-4 were prepared between 1978 and 1980. Es-14 was prepared in 1996. The materials have been in use as RM's for calibration and quality control of analytical

results in XRF analysis. The concentrations were analyzed by different laboratories and different analytical techniques for 70…77 analytes including major and trace elements, determination of Hg, H_2O^-, H_2O^+ and loss on ignition. The analytical techniques that contributed to these values were XRF, ICP-MS, ICP-OES, AES, AAS and titration [49].

Characterization of these RM's using LA-ICP-MS would allow determining if these RM's may be suitable for micro-analytical purposes.

3.2. Natural limestone CAL-S from CRPG

CAL-S is a natural limestone sample from CRPG, which was for purposes of a preliminary characterization one of the two samples that were distributed for round six of an international proficiency testing program *GeoPT* for analytical geochemistry laboratories in 1999. After conclusion of the program, values for only 3 major elements and 23 trace elements could be assigned based on data to which 63 laboratories had contributed. Analytical techniques that had contributed to these values were mostly XRF, ICP-MS, ICP-OES, AES, AAS, INAA, but also DCP-AES, gravimetric, volumetric, wet chemistry methods and titration [50].

CAL-S was analyzed as an independent natural carbonate matrix sample to compare to the other natural carbonate RM's.

3.3. Sample preparation and measurement conditions

Samples were stored in airtight plastic bags. Due to self-cementation of calcium carbonate, the particle size distribution is not expected to be stable over many years of use. Visible grains were also observed in some samples. Before sample preparation particle size distribution was measured using *Microtrac* S3500 laser diffraction analyzer with sample delivery controller. The sample was dispersed in water with *Triton* X-100 surfactant. The effect of ultrasonic treatment prior to the determination was assessed but as it did not change the particle size distribution significantly it was not included in the analytical runs. The particle size distribution curves revealed that all samples contained a notable fraction of particles larger than the laser aperture size used to ablate the samples. Particle size distribution in Es-17 before and after grinding is given in figure 3.3.1. It was concluded that it is necessary to homogenize the samples before pressing into pellets. In order to avoid possible contamination from metal parts, instead of sieving or milling the samples were ground in small portions for 4 minutes with agate mortar and pestle. We assumed that this way the

larger particle sizes are brought down to the most abundant particle size. After grinding the particle size distribution of the samples was measured again and in all cases over 95 % of the particles were smaller than 64 µm.

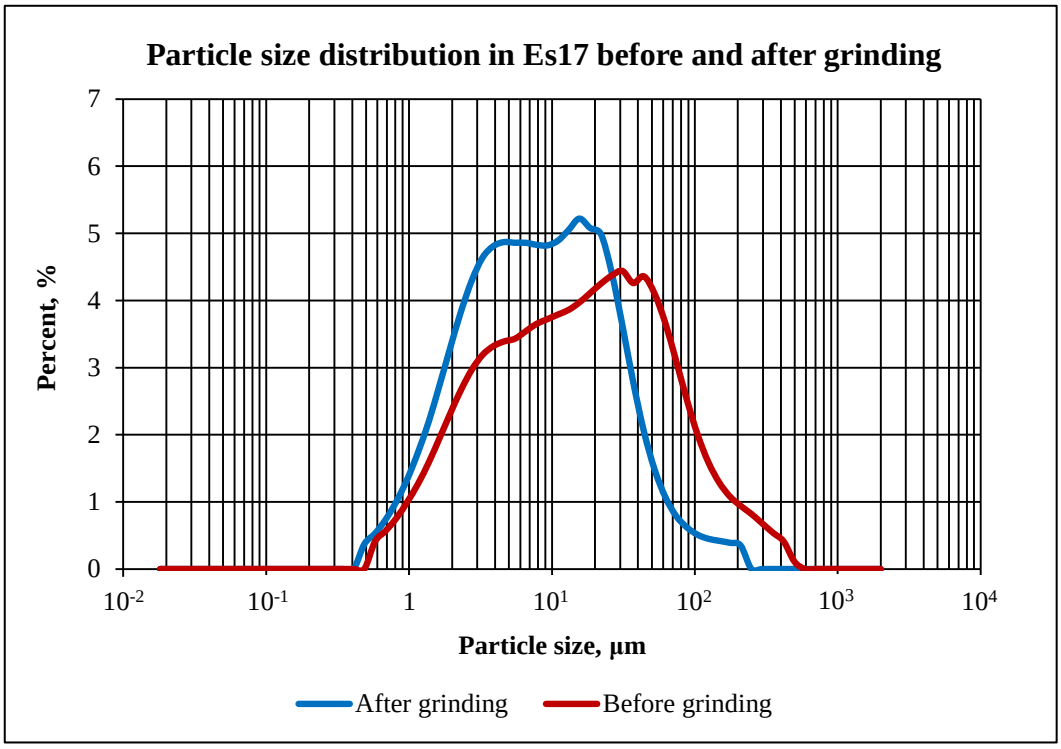

Figure 3.3.1. Particle size distribution in Es-17 before and after grinding.

After homogenization samples were pressed into pellets using a hydraulic press. The samples were pressed into aluminum holders with a diameter of 20 mm and depth of around 1 mm. Force of 15…20 kN was slowly applied and a few minutes were given for settling and was slowly released. For each sample several pellets were pressed and a preliminary ablation was performed. From these one pellet per sample was chosen that showed well defined crater edges and did not disintegrate during ablation. Comparison between an acceptable and unacceptable ablation crater is given in figure 3.3.2. Margins of the pellets were not used for analysis due to poor compaction on pressing resulting in poorly defined ablation craters. None of the pellets pressed for Es-4 exhibited well defined craters and were the most fragile out of all the pellets pressed. The anticaking properties of Es-4 may be due to the high dolomite content. The content of Ca and Mg in Es-4 is the highest while the content of all the other major elements is the lowest of all Es series RM's studied. Due to this, Es-4 was not subjected to further experiments.

The pressed samples were analyzed using *Teledyne CETAC* 213 nm Nd:YAG nanosecond laser (maximum 5 ns per pulse) ablation system LSX-213 G2+ with *HelEx*™

sample cell coupled to *Agilent Technologies* 8800 triple quadrupole ICP-MS, which was run in single quadrupole mode. Kinetic energy discrimination with 1 $mL \cdot min^{-1}$ helium flow in the collision cell was tested to lower the effect of polyatomic interferences, but was not used in the measurements as it resulted in excessive loss of signal of about an order of magnitude.

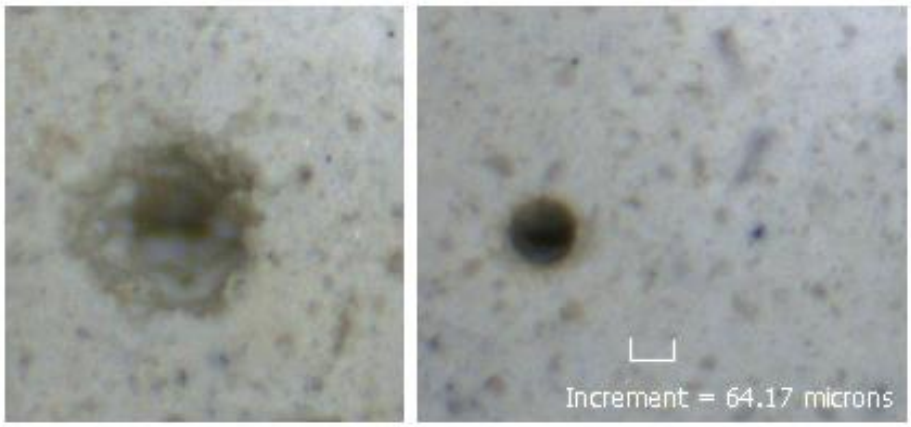

Figure 3.3.2. Optical microscope image of Es-3 pellets. Both ablation craters were created using 100 μm aperture under experimental gas flow rates. Crater on the left is considered unacceptable. Crater on the right is considered acceptable.

ICP radio frequency power was set to 1550 W. ICP-MS was tuned to liquid introduction to achieve highest signal intensity. Th^+/ThO^+ ratio was monitored as proxy of oxide formation during LA and did not exceed 0.15 % on average, indicating that oxides formed at very low level. Nebulizer argon gas flow was set to 1 $L \cdot min^{-1}$. Helium flow delivered to the sample cell was set to 0.400 $L \cdot min^{-1}$ and helium flow delivered to the sample plume collection cup was set to 0.300 $L \cdot min^{-1}$. Laser beam energy was set to 5 % with repetition rate 10 Hz and the measured fluence was 5 ± 0.55 $J \cdot cm^{-2}$. Number of laser bursts shot towards the sample surface was 500, resulting in 50 s of ablation. Wash-out time between samples was 40 s.

ICP-MS was operated in time resolved analysis mode with a dwell time of 20 ms for each of the following mass-to-charge ratios, denoted with the respective expected analytes: $^{11}B^+$, $^{23}Na^+$, $^{31}P^+$, $^{43}Ca^+$, $^{44}Ca^+$, $^{45}Sc^+$, $^{47}Ti^+$, $^{51}V^+$, $^{52}Cr^+$, $^{55}Mn^+$, $^{59}Co^+$, $^{60}Ni^+$, $^{63}Cu^+$, $^{66}Zn^+$, $^{71}Ga^+$, $^{85}Rb^+$, $^{88}Sr^+$, $^{89}Y^+$, $^{90}Zr^+$, $^{93}Nb^+$, $^{95}Mo^+$, $^{107}Ag^+$, $^{111}Cd^+$, $^{118}Sn^+$, $^{121}Sb^+$, $^{133}Cs^+$, $^{137}Ba^+$, $^{139}La^+$, $^{140}Ce^+$, $^{141}Pr^+$, $^{146}Nd^+$, $^{147}Sm^+$, $^{153}Eu^+$, $^{157}Gd^+$, $^{159}Tb^+$, $^{163}Dy^+$, $^{165}Ho^+$, $^{166}Er^+$, $^{169}Tm^+$, $^{172}Yb^+$, $^{175}Lu^+$, $^{178}Hf^+$, $^{181}Ta^+$, $^{208}Pb^+$, $^{209}Bi^+$, $^{232}Th^+$, $^{238}U^+$, resulting in total integration time of 1.117 s. Since $^{238}U^+$ was selected, the non-natural isotopic composition of U in MACS-3 and NIST 612 is not expected to influence the results significantly. $^{11}B^+$ was recorded to check the magnitude of overlap by neighboring $^{12}C^+$ spread, but no meaningful relationships could be obtained. $^{43}Ca^+$ was used as internal standard.

Analytical runs consisted of repeated analyses of samples ($N = 9$) and calibrants. Each sequence was analyzed at 40 μm (round), 65 μm (square) and 100 μm (round) spot diameters. Calibrants were analyzed in each run in the beginning, middle and end.

For calibration silicate glass NIST 612 and synthetic calcium carbonate MACS-3 was used. Reference values for NIST 612 established by Jochum et al. (2011) at different test portion masses were used [6]. Reference values for MACS-3 from the preliminary certificate with concentrations based on analysis by USGS were used, except the value for Nb, for which a working value suggested by Chen et al. (2011) was used [51]. Natural limestone CAL-S was included in the analytical run for overall comparison with other natural carbonate matrices.

3.4. Data processing

MassHunter software (*Agilent Technologies*, USA) was used for controlling ICP-MS and recording signals. For time resolved signal processing *GLITTER* software (*GEMOC* National Key Centre, Australia) was used. It provides the signal integration and calibration functionality, and also one sigma error estimate for each element in a determination using counting statistics applied to time resolved signal and background. Considering the very low number of outliers encountered in analysis of certified reference materials, the time resolved signals were not filtered in *GLITTER*, because filtering could impose a "false" homogeneity. *GLITTER* estimates the minimum detection limit at 99 % confidence level using the background count rates.

Concentrations and uncertainties calculated with *GLITTER* were exported and processed using *Excel* (*Microsoft*, USA) and statistics package *MYSTAT* (*Systat*, USA). After treatment of outliers element concentrations were calculated as averages of all determinations.

3.5. Treatment of outliers

In order to eliminate extreme outlying values, which may have occurred due to random disturbances, the concentration values beyond three standard deviations from the median were excluded. Different elimination criteria were tested and it was observed that the agreement between element concentrations from bulk analyses and the determined LA-ICP-MS values worsened if too many outliers were removed, therefore three standard deviations from the median was chosen as the criterion. A small number of outliers at this level (<0.7 %) was excluded from further analysis from data calibrated to both of calibration RM's, this exclusion did not lead to significant loss of degrees of freedom.

The concentration data after outliers elimination were tested for normal distribution using Shapiro-Wilk test at significance level α=0.05. The null hypothesis states that the data follows normal distribution. For most cases, the p values were p>0.05, thus the hypothesis could not be rejected. The data could not be further improved by exclusion of outliers, because there is evidence that elimination leads to bias, thus a "false" homogeneity would be imposed. Therefore the variables, which did not follow normal distribution, were analyzed further.

3.6. Uncertainty estimation

The uncertainty of a determination of concentration from repeated measurements is often estimated simply as the experimental standard deviation of the mean as shown in equation 3.6.1.

$$u_{rep} = \frac{s_{exp.}}{\sqrt{N}} \qquad (3.6.1)$$

where u_{rep} – uncertainty of repeatability;

$s_{exp.}$ – experimental standard deviation of measurements;

N – number of measurements.

This estimation is useful when the analyzed material is sufficiently homogenous at the analyzed test portion size. While it is recognized that significant inhomogeneity will be reflected in this uncertainty estimation, the uncertainty due to inhomogeneity does not decrease as the number of measurements increases [38]. Most laboratories usually attempt homogenization rather than evaluate inhomogeneity separately [52]. Microanalysis likely could detect inhomogeneity in materials that are considered sufficiently homogenous, especially if the material is not designed for micro-analytical purposes, therefore inhomogeneity should be quantified separately.

For certified uncertainty IAG protocol suggests the use of a combined uncertainty from interlaboratory programmes as shown in equation 3.6.2, where an additional component of uncertainty due to inhomogeneity is added whenever two or more contributing laboratories detect inhomogeneity.

Small inhomogeneity, even if not statistically significant, should be accounted for in the uncertainty of the certified value [38]. It is suggested that detection of small inhomogeneity is preferable to finding of homogeneity [39].

$$u_c = \sqrt{\frac{s_{labs}}{\sqrt{N_{labs}}} + u_{inhom.}^2 + u_{dry\ wt.}^2 + u_{bias.}^2} \quad (3.6.2)$$

where u_c – combined standard uncertainty;

N_{labs} – number of participating laboratories;

$u_{inhom.}$ – uncertainty due to material inhomogeneity;

$u_{dry\ wt.}$ – uncertainty in dry weight;

s_{labs} – standard deviation of concentration data from all laboratories;

u_{bias} – uncertainty due to bias between procedures.

In this case there are no multiple laboratories, uncertainty in dry weight is considered insignificant and no estimation of bias can be performed, because a suitable CRM, which is not used for calibration of this procedure, is not available. Therefore the uncertainty estimated for the determined concentration value in our candidate RM is determined by equation 3.6.3, where specific components are added to account for uncertainty in internal standard concentration and reference value. The uncertainty due to measurement procedure and uncertainty due to inhomogeneity are quantified separately. In this case the inhomogeneity that can be detected using the measurement procedure is included in the combined uncertainty even if it is not statistically significant.

Student's t-distribution was used to assign the coverage factor k at 95 % confidence level in order to estimate the expanded uncertainty, as shown in equation 3.6.4.

$$u_c = \sqrt{\left(\frac{u_{meas.}}{\sqrt{N}}\right)^2 + u_{inhom.}^2 + u_{IS}^2 + u_{RMC}^2} \quad (3.6.3)$$

where u_c – combined standard uncertainty;

$u_{meas.}$ – uncertainty due to measurement procedure;

N – number of measurements;

u_{IS} – uncertainty in values of the internal standard;

u_{RMC} – uncertainty in values of the calibration RM.

$$U_{95\,\%} = k \cdot u_c \quad (3.6.4)$$

To evaluate agreement between the results and available reference values the normalized error test (E_n number) was used, as shown in equation 3.6.5. E_n number equal

to 1.0 or below is usually interpreted as an acceptable agreement between values. E_n number greater than 1.0 is usually interpreted as unacceptable disagreement between values.

$$E_n = \frac{x - x_{ref}}{\sqrt{U_x^2 + U_{x_{ref}}^2}} \tag{3.6.5}$$

where x – determined value;

x_{ref} – reference value;

U_x – expanded uncertainty of determined value;

$U_{x_{ref}}$ – expanded uncertainty of reference value.

3.7. Homogeneity testing

Homogeneity testing should be performed with methods that are more precise than the target uncertainty of candidate RM. Potential difference between test portion masses should be checked for candidate micro-analytical RM's. For evaluation of homogeneity of candidate RM's using LA-ICP-MS the measurements of element concentrations in both the calibration RM and candidate RM should be performed with sufficient number of measurements and within temporal proximity to reduce the impact of drift and other possible effects that become random over a long period of time. Measures must be taken to detect and correct for drift especially if the purpose includes finding possible trends in homogeneity, e.g., trends between core and rim part of a RM, bottom to top, etc. [37], [38], [44].

In principle the internal standardization could correct for matrix effects, ablated amount and instrumental drift, provided that there is no significant interference affecting the mass-to-charge ratio of both analyte and internal standard, and the internal standard closely matches the chemical and physical properties of analyte, but this is rarely the case. In geological samples the major elements that could be accurately quantified beforehand and are suitable as internal standards usually are of low atomic mass. Therefore the sensitivity of each analyte may change relative to the internal standard during analysis, thus the internal standard in geological samples analyzed using LA-ICP-MS usually is not fully effective for correcting matrix effects and drift. Due to these problems with internal standardization, for reliable quantification and correction for drift a sufficiently homogenous matrix matched RM with low uncertainties should be used [36].

Concentration data obtained within a single day were LOD filtered and the data scaled by dividing each case with its respective mean value to analyze the relative variances. A small

number of outliers (<0.7 %) were excluded from further analysis, using three standard deviations from the median criterion, and this exclusion did not lead to significant loss of degrees of freedom. As concluded in 3.5, elements affected by enriched or depleted areas are not homogenous and the outlying values are part of true material inhomogeneity.

Cases were tested for normal distribution using Shapiro–Wilk test and skewness and standard error of skewness was calculated. Ratio of skewness to standard error of skewness of more than 2 suggests significant skewness, which was true for most non-normal data. Majority of cases were distributed normally.

All analyzed materials were compared pairwise to MACS-3. This way the uncertainties due to measurement procedure cancel out to a large extent. To determine whether differences in relative experimental standard deviations are statistically significant, statistics software *MYSTAT* was used to perform pairwise variance comparisons using the F-test for equality of two variances at significance level α=0.05. The null hypothesis states that samples come from populations with equal variances. If p>0.05 the hypothesis could not be rejected. The smaller the p-value the stronger is the evidence against the hypothesis. F-test results where the sample to be compared to MACS-3 had less than 3 repeated measurements were removed.

Homogeneity indices H, as shown in equation 2.6.10, were estimated for all elements for all reference materials. Uncertainty due to counting process during detection $u_{Pois.i}$ was estimated with *GLTITER* software used for data reduction, as shown in equation 3.7.1.

$$u_{Pois.i} = \frac{\sigma_{Pois.i}}{\sqrt{N}} \tag{3.7.1}$$

where $\sigma_{Pois.i}$ – the one sigma error estimate i from *GLITTER* software;

N – number of measurements.

The homogeneity indices for P, Rb and Cs were estimated using values calibrated to NIST 612, because no concentration values are given for these elements in MACS-3.

Hypothesis tests discussed previously are merely comparative and can be used to confirm or reject statistically significant inhomogeneity, however, to be able to include uncertainty due to inhomogeneity in the certified combined uncertainty it should be quantified and was done according to equation 2.6.11. It has been suggested that small inhomogeneity, even if not statistically significant, should be included in the uncertainty of certified value [38].

4. RESULTS AND DISCUSSION

4.1. Element concentrations

Despite matrix mismatch, the determined values, taking into account the expanded uncertainty, for MACS-3 calibrated to NIST 612 show good agreement between the reference values for almost all elements. The agreement for Sb at all spot diameters was not acceptable and the agreement of P, Rb and Cs could not be evaluated, because there are no values given for these elements in MACS-3. Determined concentrations, expanded uncertainty and E_n numbers for MACS-3 calibrated to NIST 612 are given in table 8.5 in appendix 2. This gives an idea of the quality of measurements and uncertainty estimation.

The determined concentrations showed good agreement with reference values from bulk analysis methods on the candidate RM's, except for Es-3, where Co, Cu and some REE's (Eu, Tb, Ho, Tm, Lu and Th) fell out of agreement. Measurements of Co and Cu were significantly lower than reference values, but measurements of the REE's were significantly higher. Measurements of Zr fell out of agreement for several candidate RM's and were significantly lower. This discrepancy is likely due to dispersed zircon grains present in the RM's. Due to physical hardness, these grains can resist the milling and are not evenly distributed on microscale. Measurement of Co fell out of agreement with the reference values for CAL-S and was significantly lower. These disagreements had E_n numbers higher than 1.4. E_n number of less than 0.94 means that more than 33 % of expanded uncertainty ranges of the values overlap. E_n number above 1.41 means that the expanded uncertainty ranges do not overlap at all. The disagreement of concentrations of REE's in Es-3 may have occurred by chance due to the limited number of measurements.

For purposes of determination of CRM reference values, LA-ICP-MS is not the best method in terms of accuracy. The determined concentrations, expanded uncertainties and E_n numbers together with reference values and uncertainties are given in table 8.5-8.11 in appendix 2.

4.2. Evaluation of homogeneity

Different approaches to evaluation of homogeneity were used: pairwise F-tests between candidate RM and a homogenous reference material, calculation of homogeneity indices and quantification of the uncertainty due to inhomogeneity. These approaches answer essentially different questions. Pairwise F-tests determine whether there is statistically significant

difference between candidate RM and the homogenous reference material. In this approach the uncertainties due to measurement procedure cancel out, at least to a large extent, but the homogenous reference material then sets the benchmark for homogeneity. Homogeneity indices allow determining whether inhomogeneity could be suspected based on the estimate of uncertainty due to measurement procedure, which is a metrologically sound approach as opposed to looking at experimental RSD's, because a high RSD does not necessarily mean the element is inhomogeneous. This is especially true for elements near LOD, because those always have higher experimental RSD's, but the estimate of uncertainty due to measurement procedure is also higher.

P-values from the F-tests performed pairwise to MACS-3 are given in table 4.2.3. F-tests for P, Rb and Cs were performed on mean count rates relative to internal standard after scaling, because no concentration values are given in MACS-3. P-values in bold-italic represent a comparison where the element in sample compared to MACS-3 had a lower variance, values in red represent comparison where the element in one of the samples was not normally distributed, and thus the result should be treated with caution. Unless variance of an element is less than that of MACS-3, p-values less than 0.05 are not shown. The higher is the p-value, the stronger the evidence that the difference is not statistically significant.

Almost all outliers were values elevated with respect to the average element concentration and were distributed randomly across the concentration data. Some samples had more outliers than on average, indicating that an area enriched in some elements had been ablated. A visual representation of the ablation profiles of a sample during trial ablation containing an area with elevated concentrations of some REE's is shown in figure 4.2.1. However, such areas of elevated concentration were not so well defined in all ablation profiles. All cases of elevated concentrations were examined and it was found that in several cases the outlying elements occurred in groups, most obviously the REE's, while Y, Zr, Nb, Mo, Ag, Cd, Sn, Sb and Ga, Rb, and Ti, V, Cr, Mn, Co, Ni occurred together in smaller groups. Outliers occurring together were detected in natural carbonate RM's and were much less common in MACS-3 and NIST 612. The 25 replicates with more than two times the average number of outliers were found out of the total 342 cases and are given in table 8.4 in appendix 1. Outliers up to three standard deviations should not be removed as was considered previously, because they are a part of the true inhomogeneity of the materials.

The elevated number of outliers occurring together and the frequency at which they occur can serve as an overall indication of inhomogeneity, providing that statistical significance is reached. Empirical probability of finding more than two times the average

number of outliers occurring together in a replicate based on two standard deviations from the median at any spot diameter was estimated for each sample, and is given in table 4.2.1.

Outlier detection based on 2*s* from the median showed that REE's were frequently found as a group of outliers. This serves as evidence of possible inhomogeneity of REE's in these samples. Although not very reliable due to the limited number of measurements, the empirical probabilities of finding two times the average number of outliers occurring together serves as an indicator of the abundance of particles enriched in some elements. These probabilities showed that Es-14 and Es-18 are likely to be very inhomogeneous, which is confirmed by the relative uncertainties of inhomogeneity. Probabilities for other samples were not significantly different from MACS-3, except NIST 612 and Es-3, which were the lowest. Time resolved signals for Es-17 during a trial ablation showed a particle rich in REE's.

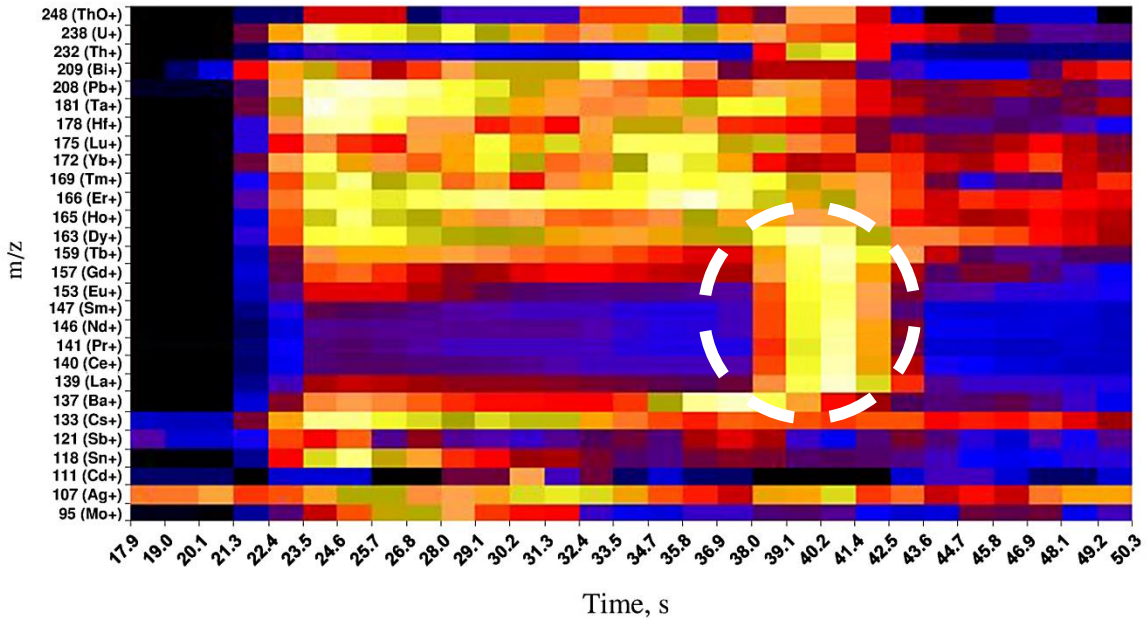

Figure 4.2.1. Plot of time resolved signals for Es-17. Lighter colors indicate higher count rates with respect to the rest of signal. Area greatly enriched in Ba, La, Ce, Pr, Nd, Sm, Eu, Gd, Tb and Dy is circled.

Estimated homogeneity indices H are given in table 4.2.4. Criterion of $H \leq 3$ for confirming homogeneity was used. Values of $H > 3$ are marked in red. The results from pairwise comparisons and estimated homogeneity indices are similar. The criterion of $H \leq 3$ for confirming homogeneity proved stricter than the hypothesis testing by F-tests, because it resulted in excluding elements that gave p-values just slightly above 0.05 (cutoff p-value of approximately 0.14 determined from comparing tables 4.2.3 and 4.2.4). Criterion of $H \leq 4$ would include these elements with p-values slightly above 0.05 as well. Therefore with $H \leq 3$ only elements with strong evidence supporting homogeneity would be confirmed as

homogenous. For Cs and Rb significant inhomogeneity can be detected in MACS-3. Cs and Rb were found to be more homogenous in Es-17, Es-3 and Es-16 than in MACS-3 and the concentrations of Rb and Cs are higher in the candidate RM's. P was found to be more homogenous in CAL-S, Es-14, Es-17 and Es-3 than in MACS-3.

$u_{inhom.}$ at each spot diameter is given in table 8.1, 8.2 and 8.3 in appendix 1. Relative uncertainties of inhomogeneity in CAL-S, NIST 612 and MACS-3 at different spot diameters are averages from 3 analytical runs performed on different days. For quantification of $u_{inhom.}$ on few occasions where the uncertainty assumed a negative value under the square root, the experimental standard deviation was used as estimate of $u_{inhom.}$.

Magnitude of maximum relative $u_{inhom.}$ at spot diameters 40 µm...100 µm is given in table 4.2.2 grouped according to arbitrary criteria. For Cs, Rb and P values calibrated to NIST 612 were used, because no concentration values are given in MACS-3.

The relative uncertainties due to inhomogeneity, as shown in table 8.1-8.3 in appendix 1, show that NIST 612 is the most homogenous material analyzed, followed by MACS-3 and the other natural limestone and dolomite samples being the most inhomogeneous. To illustrate the difference between NIST 612, MACS-3 and the natural limestone and dolomite RM's the distribution of elements among different ranges of uncertainty due to inhomogeneity is plotted in figure 4.2.2. It can be seen that out of the natural samples Es-16 and Es-17 exhibit the largest number of elements with relative uncertainty values comparable to NIST 612 and MACS-3.

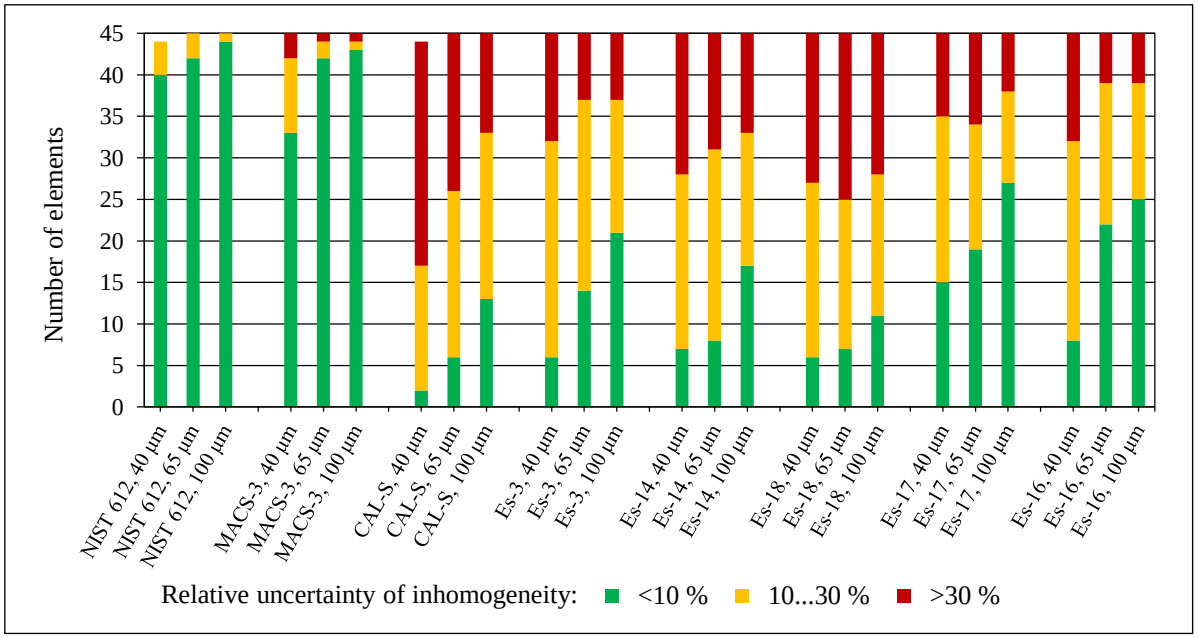

Figure 4.2.2. Stack plot representing the distribution of elements among different ranges of relative uncertainties due to inhomogeneity at different spot diameters for each RM.

Table 4.2.1. Empirical probabilities of finding more than two times the number of outliers than on average occurring together in a replicate based on 2*s* from the median value.

Sample	$P = n_{observed}/n_{total}$
NIST 612	0.01
Es-3	0.04
CAL-S	0.06
MACS-3	0.07
Es-17	0.07
Es-16	0.07
Es-14	0.18
Es-18	0.21

Table 4.2.2. Summary of inhomogeneity drawn from the maximum relative $u_{inhom.}$ at spot diameters 40 µm...100 µm. Elements with detectable inhomogeneity as evidenced by the homogeneity indices marked in red.

	Homogenous $u_{inhom.} < 10$ %	Moderately inhomogenous $u_{inhom.} = 10 \ldots 30$ %	Grossly inhomogenous $u_{inhom.} > 30$ %
NIST 612	Na, Ca, Sc, Ti, V, Mn, Co, Ni, Cu, Zn, Ga, Rb, Sr, Y, Zr, Ag, Cd, Cs, Ba, La, Ce, Pr, Nd, Sm, Eu, Gd, Tb, Dy, Ho, Er, Tm, Yb, Lu, Hf, Ta, Pb, Th, U.	P, Cr, Nb, Mo, Sn, Sb, Bi.	
MACS-3	Na, Ca, Sc, Ti, Cr, Co, Ni, Cu, Zn, Ga, Sr, Y, Zr, Nb, Cd, Sn, Sb, Ba, La, Pr, Sm, Eu, Gd, Tb, Dy, Ho, Er, Tm, Yb, Lu, Hf, Ta, Th.	V, Mn, Mo, Ag, Ce, Nd, Pb, Bi, U.	P, Rb, Cs.
CAL-S	Y, La.	Na, P, Ca, Sc, V, Cr, Mn, Sr, Cd, Ba, Pr, Nd, Ho, U.	Ti, Co, Ni, Cu, Zn, Ga, Rb, Zr, Nb, Mo, Ag, Sn, Sb, Cs, Ce, Sm, Eu, Gd, Tb, Dy, Er, Tm, Yb, Lu, Hf, Ta, Pb, Bi, Th.
Es-14	Ca, Ga, Sr.	Na, P, Sc, V, Mn, Rb, Y, La, Ce, Sm, Eu, Gd, Dy, Ho, Tm, Lu, U.	Ti, Cr, Co, Ni, Cu, Zn, Zr, Nb, Mo, Ag, Cd, Sn, Sb, Cs, Ba, Pr, Nd, Tb, Er, Yb, Hf, Ta, Pb, Bi, Th.
Es-18	Ca, V, Sr.	Mn, Co, Ni, Zn, Ga, Nb, Cd, Cs, Tb, Dy, Er, Yb.	Na, P, Sc, Ti, Cr, Cu, Rb, Y, Zr, Mo, Ag, Sn, Sb, Ba, La, Ce, Pr, Nd, Sm, Eu, Gd, Ho, Tm, Lu, Hf, Ta, Pb, Bi, Th, U.
Es-17	Ca, Sc, Sr, La, Pr, Nd, Eu, Th.	Na, P, Ti, V, Cr, Mn, Co, Ni, Zn, Ga, Rb, Zr, Nb, Cs, Sm, Tb, Yb, Lu, Hf, Bi, U.	Cu, Y, Mo, Ag, Cd, Sn, Sb, Ba, Ce, Gd, Dy, Ho, Er, Tm, Ta, Pb.
Es-3	Ca, La, Pr, Nd.	P, Sc, V, Cr, Mn, Co, Zn, Ga, Rb, Y, Cd, Sn, Cs, Sm, Eu, Tb, Dy, Ho, Er, Tm, Yb, Lu, Hf, Th, U.	Na, Ti, Ni, Cu, Sr, Zr, Nb, Mo, Ag, Sb, Ba, Ce, Gd, Ta, Pb, Bi.
Es-16	Ca, Mn, Rb, Y, La, Pr, Tb, Er.	Sc, Ti, V, Co, Ga, Nb, Sb, Cs, Ba, Nd, Sm, Eu, Gd, Dy, Ho, Tm, Yb, Lu, Hf, Th, U.	Na, P, Cr, Ni, Cu, Zn, Sr, Zr, Mo, Ag, Cd, Sn, Ce, Ta, Pb, Bi.

Table 4.2.3. P-values from F-tests performed on NIST 612, CAL-S, Es-14, Es-18, Es-3, Es-17 and Es-16 pairwise to MACS-3 for each element. P-values in bold-italic represent a variance for the element lower than in MACS-3. Values in red indicate deviations from normal distribution.

	NIST612			CAL-S			Es-14			Es-18			Es-3			Es-17			Es-16		
Element	40 µm	65 µm	100 µm	40 µm	65 µm	100 µm	40 µm	65 µm	100 µm	40 µm	65 µm	100 µm	40 µm	65 µm	100 µm	40 µm	65 µm	100 µm	40 µm	65 µm	100 µm
Na	***0.014***	***0.046***	***0.043***				0.986									0.095					0.246
P		0.232	***0.239***				0.168	0.142	***0.001***		0.570	***0.114***	***0.021***						***0.032***	0.992	0.243
Ca	***0.150***	***0.067***	***0.268***	0.984	0.958	0.959	***0.001***	***0.612***	0.598	***0.227***	***0.223***	0.551	***0.218***	***0***	***0.003***	0.918	***0.373***	***0.423***	***0.523***	***0.119***	0.356
Sc	***0.033***	0.720	0.513				0.083		0.073				0.071		0.081	0.487	0.160			0.559	0.464
Ti	***0.218***	***0.035***	0.837													***0.521***			0.254		
V	***0.008***	0.320	0.703	0.333	***0.358***		***0.690***		0.205	***0.482***	0.171	0.842	***0.416***			***0.903***	0.810	0.982	0.053	***0.348***	0.510
Cr	***0.268***	0.109	0.965	0.143						0.081	0.266	***0***	0.199	***0.210***		0.416	***0.890***	0.104		0.087	
Mn	***0.164***	0.992	0.068	***0.063***	0.907		0.171	0.611		0.536	***0.341***		0.289	0.292		***0.379***			***0.686***	***0.269***	0.797
Co	***0.223***	0.281	***0.056***							0.229			0.089				0.134	0.058	0.164		
Ni	***0.008***	0.282	0.859				0.119			***0.564***										0.216	
Cu	***0.081***	***0.185***	0.250																		
Zn	***0.389***	0.505	0.147	0.784	0.948					0.109				0.190			***0.268***		0.340	0.116	
Ga	***0.184***	0.640	***0.187***				***0.601***	0.100	0.344	0.111			0.349	0.259		0.276	0.350	0.974		***0.759***	***0.427***
Rb	***0***	***0***	***0***	0.509	0.425	***0.947***	***0.211***	***0***	***0***	0.980	***0.045***	***0.001***	0.876		***0.124***	0.924		***0.006***		***0.167***	***0***
Sr	***0.038***	***0.001***	***0.018***	0.307	***0.210***	0.934	***0.321***	***0.779***	0.446	***0.489***	***0.705***	0.511		0.974	0.401	***0.736***	0.734	0.340		0.781	***0.216***
Y	***0.003***	0.096	***0.162***	0.776	***0.487***	***0.660***	0.687			0.327						***0.512***		0.552	0.369	0.866	0.480
Zr	***0.078***	0.242	***0.039***										0.051			0.275					
Nb	***0.499***	***0.064***	***0.107***													0.055					
Mo	***0.003***	***0.067***	***0.039***	***0.979***									0.054							0.070	
Ag	***0.012***	***0.477***	***0.035***																		
Cd	***0.264***	0.844	0.914																		
Sn	***0.012***	0.684	0.635																		
Sb	***0.066***	***0.202***	***0.238***				0.194														
Cs		***0***	***0***					***0.001***	***0***		***0***	***0***			***0.078***			***0.015***		0.681	***0.001***
Ba	***0.149***	***0.820***	***0.212***											0.056					0.084	0.228	
La	***0.089***	***0.081***	***0.203***	***0.717***	0.864	0.677			0.070				0.638	0.262		0.393	0.503	0.082	0.336	0.708	0.404
Ce	***0.026***	0.818	***0.001***				0.651		0.359												
Pr	***0.053***	***0.131***	0.861	0.269					0.126				0.671	0.156		0.913	0.074		***0.893***	0.551	0.630
Nd	***0.011***	***0.133***	0.975										***0.650***	0.070		***0.253***	0.361	0.562	0.173	0.208	0.907
Sm	***0.163***	***0.109***	0.928						0.683				0.130			0.256	0.121		0.074	0.243	
Eu	***0.102***	***0.219***	0.827				***0.928***		0.156				0.722			0.843			0.057	0.319	0.061
Gd	***0.062***	0.769	***0.002***				0.384												0.093		
Tb	***0.214***	0.919	0.808													0.574			0.950	0.331	0.099
Dy	***0.024***	0.621	***0.375***				0.552			0.412			0.062			***0.295***			0.321	***0.785***	0.835
Ho	***0.072***	0.888	***0.158***				0.059			0.869										0.574	0.850
Er	***0.060***	0.751	0.922				0.321			***0.672***						0.362			0.174	0.613	0.991
Tm	***0.086***	***0.263***	0.931	***0.836***			0.254												0.235	0.122	0.333
Yb	***0.023***	***0.860***	0.862				0.257						0.127			***0.438***			0.134	0.950	***0.330***
Lu	***0.026***	0.985	0.446													0.269				0.426	***0.404***
Hf	***0.029***	***0.061***	0.879										0.051						0.050		
Ta	***0.004***	0.976	***0.193***													0.064					
Pb	***0.002***	***0.396***	***0.007***																		0.803
Bi	***0.005***	0.702	***0.029***																		
Th	***0.072***	***0.328***	0.467				***0.503***			0.412			0.711			0.725	0.614				
U	***0.023***	***0***	***0.001***	***0.616***	***0.094***	***0.029***	***0.047***	0.467	0.173	***0.114***	0.069		***0.085***	***0.622***	0.365	0.277	***0.228***	***0.098***	***0.019***	0.880	0.187

Table 4.2.4. Homogeneity indices H estimated from MACS-3, CAL-S, Es-14, Es-18, Es-3, Es-17 and Es-16. Values of $H > 3$ marked in red.

	MACS-3			CAL-S			Es-14			Es-18			Es-3			Es-17			Es-16		
Element	40 µm	65 µm	100 µm	40 µm	65 µm	100 µm	40 µm	65 µm	100 µm	40 µm	65 µm	100 µm	40 µm	65 µm	100 µm	40 µm	65 µm	100 µm	40 µm	65 µm	100 µm
Na	1.4	1.4	1.4	3.3	5.8	6.9	2.2	6.0	9.3	7.5	6.1	11.5	7.3	4.8	17.1	3.7	9.1	4.0	17.4	26.8	3.2
P	0.2	1.5	1.9	0.5	6.6	1.6	0.3	1.3	0.7	0.0	0.8	1.0	0.2	0.5	1.1		1.2	2.0	0.1	0.5	0.4
Ca	1.4	1.4	1.3	1.3	1.5	1.8	0.6	1.5	1.5	1.1	0.9	1.0	0.9	0.3	0.4	2.0	1.4	1.4	1.8	1.1	1.4
Sc	1.4	1.3	1.4			2.0	2.8	4.3	3.6	2.5	17.3	6.5	2.3	3.5	2.4	2.0	2.9	4.1	4.6	2.5	1.4
Ti	1.1	1.4	1.3	4.4	6.5	10.1	6.0	8.7	11.1	4.8	14.1	4.9	3.1	10.4	3.8	1.5	5.0	7.5	3.2	8.2	10.8
V	1.4	1.4	1.3	2.3	2.3	3.4	1.5	6.4	2.9	1.1	2.4	1.3	1.0	3.1	3.5	1.7	2.0	1.8	5.2	1.5	2.6
Cr	1.3	1.2	1.2	2.0	3.2	6.2	7.5	20.4	4.0	3.0	2.1	9.1	2.2	0.8	3.0	2.5	1.7	3.4	4.9	4.3	13.8
Mn	1.2	1.3	1.4	2.0	1.3	3.5	3.3	2.3	6.1	1.9	1.0	2.9	2.0	2.2	15.8	1.4	5.9	15.0	1.7	1.3	1.9
Co	1.3	1.3	1.4	4.2	5.6	5.3	6.4	15.8	7.0	2.2	8.5	3.7	2.4	9.1	10.8	4.3	3.0	3.7	3.9	5.1	5.9
Ni	1.2	1.2	1.3	4.6	7.9	16.6	3.4	25.5	6.3	1.1	6.8	5.9	3.0	15.6	5.3	5.7	4.6	11.6	5.2	3.1	8.7
Cu	1.2	1.3	1.4	3.1	5.4	17.7	4.2	38.5	9.7	3.3	11.4	23.9	8.3	3.0	6.4	11.7	7.1	22.2	6.5	16.0	10.1
Zn	1.3	1.3	1.4	1.7	1.5	4.7	5.9	2.3	47.0	2.3	3.5	4.2	4.0	2.5	9.3	4.3	1.4	5.4	3.0	4.1	60.7
Ga	1.2	1.3	1.3			4.7	1.4	3.3	2.6	2.4	3.5	4.0	1.9	2.0	3.2	2.8	2.6	1.8	2.7	1.7	1.4
Rb			46.4	2.0	1.7	5.4	5.5	2.4	5.8	10.3	4.0	13.9	3.8	5.1	3.8	4.0	7.5	2.6	1.4	1.5	1.5
Sr	1.3	1.3	1.3	1.7	1.0	1.6	1.3	1.7	2.5	1.1	1.0	1.6	5.8	1.5	1.6	1.7	1.8	2.7	9.5	2.3	1.2
Y	1.3	1.3	1.4	1.3	2.2	1.7	2.1	34.0	5.6	2.0	33.1	8.5	4.2	11.0	4.9	1.5	20.7	2.3	3.0	2.2	2.8
Zr	1.3	1.3	1.3	11.0	10.8	16.5	4.8	8.6	31.1	3.7	0.1	10.0	2.7	5.6	13.2	2.7	13.2	11.7	10.7	9.7	21.2
Nb	1.3	1.3	1.3	4.1	8.6	8.5	6.5	12.8	22.5	3.3	9.5	8.3	4.2	12.1	21.1	3.7	10.8	4.1	4.9	11.1	5.5
Mo	1.5	1.3	1.3	0.7	3.1	8.0	4.0	9.3	6.5	2.1	9.9	3.4	2.5	6.5	6.8	9.4	11.9	21.2	6.0	2.8	3.2
Ag	1.3	1.2	1.3				6.1	22.7	15.1			1.3	3.0	6.0	4.5						2.3
Cd	1.1	1.3	1.4		3.4	2.9	10.7	32.4	8.1	1.7		3.7	2.7	1.2	3.5	3.2	9.5	3.6	1.7	4.5	2.2
Sn	1.3	1.3	1.3	2.1	10.3	14.5	8.4	10.7	16.2	3.8	7.0	2.8	3.2	5.3	13.9	5.0	3.9	4.3	7.5	4.6	6.4
Sb	1.2	1.2	1.3	7.6	4.4	7.6	2.9	11.8	18.1	2.6	3.3	8.4	4.1	10.1	10.8	3.9	5.3	39.0	3.4	3.6	3.7
Cs			24.4				9.0	4.2	5.1	3.9	2.5	5.0	3.0	4.3	5.4	2.8	7.6	4.6	1.5	1.0	1.7
Ba	1.2	1.3	1.3	4.0	8.9	8.5	4.4	16.5	11.3	8.1	13.2	11.9	12.0	2.8	17.5	6.9	11.6	8.2	4.3	3.4	8.6
La	1.3	1.3	1.4	1.5	1.7	1.9	0.0	6.8	3.8	4.6	18.2	40.0	1.7	2.1	5.6	2.6	2.4	3.6	3.1	2.5	2.9
Ce	1.3	1.3	1.3	6.7	9.2	5.2	2.2	4.2	2.6	3.9	13.7	3.5	2.7	22.2	15.9	4.7	13.7	13.6	10.4	10.6	21.7
Pr	1.3	1.4	1.4	2.3	3.4	3.1	12.3	5.7	3.3	4.9	3.6	4.3	1.6	2.5	6.5	2.0	3.8	4.6	2.0	2.8	2.5
Nd	1.2	1.4	1.4	4.1	3.1	3.5	4.5	7.1	8.0	4.3	10.2	8.1	1.2	2.7	4.6	1.2	2.6	2.3	3.6	3.7	2.1
Sm	1.3	1.4	1.4	3.1	3.2	4.2	5.7	5.7	1.9	6.6	7.8	3.2	2.1	2.8	5.6	2.5	3.0	4.3	4.1	3.4	5.1
Eu	1.3	1.4	1.4	2.3	2.8	5.1	1.6	5.5	2.3	5.7	5.6	38.1	1.5	5.6	9.2	1.9	5.1	4.5	4.5	3.1	4.4
Gd	1.3	1.4	1.4	1.5	2.6	4.0	2.4	10.9	3.9	0.9	5.9	23.0	4.3	12.0	12.5	6.7	20.4	15.7	4.1	9.4	10.2
Tb	1.3	1.4	1.4	3.4	2.5	5.6	4.0	11.9	4.4	2.9	5.4	2.1	4.3	4.0	4.9	2.0	12.6	3.9	2.0	3.2	4.0
Dy	1.3	1.3	1.4	3.2	3.6	2.7	2.1	5.0	4.9	1.7	9.8	2.6	2.6	3.4	5.1	1.2	15.1	4.4	2.9	1.7	2.2
Ho	1.3	1.4	1.4	3.1	2.8	4.1	3.2	16.3	6.4	1.3	19.1	14.3	2.6	3.5	3.8	3.4	16.1	3.7	3.9	2.5	2.1
Er	1.2	1.3	1.4	3.2	6.0	2.3	2.5	24.5	7.4	1.2	4.4	7.7	3.1	4.5	3.5	2.4	14.5	3.6	2.1	2.5	1.9
Tm	1.3	1.3	1.4	2.3	3.9	6.1	2.2	6.5	9.2	0.2	19.6	18.6	4.6	5.5	8.3	3.6	16.2	4.2	2.7	3.4	2.7
Yb	1.3	1.4	1.4	1.3	1.9	1.9	2.1	11.7	9.1	3.0	2.0	9.8	2.1	4.0	6.3	1.2	1.4	6.8	3.2	1.9	1.3
Lu	1.3	1.4	1.4	2.4	6.3	4.3	2.9	10.0	11.3	2.9	30.0	15.0	3.5	3.3	8.2	1.8	8.4	7.4	3.6	2.6	1.3
Hf	1.3	1.3	1.4	6.9	4.6	6.8	3.4	23.6	45.2	5.2	0.5	2.8	2.2	6.6	6.0	1.7	9.5	8.4	3.2	4.5	12.6
Ta	1.2	1.4	1.4		4.5	5.9	4.7	8.5	37.7	3.2	5.2	9.4	5.9	9.1	9.1	3.1	6.6	16.6	5.0	7.2	14.3
Pb	1.3	1.3	1.3	4.2	7.0	7.0	8.5	15.3	7.7	4.1	7.6	11.2	3.7	13.8	16.0	10.0	10.2	15.5	15.2	21.3	2.3
Bi	1.3	1.2	1.3			9.1	7.5	16.2	12.5	2.8	8.8	6.6	6.9	6.5	4.2	6.7	5.9	4.9	5.8	6.3	4.3
Th	1.3	1.4	1.4	4.7	6.2	7.5	10.6	10.3	7.4	1.9	24.6	2.1	1.5	6.3	6.6	2.1	2.3	5.6	7.2	7.2	5.4
U	1.3	1.3	1.3	0.4	0.7	0.9	0.9	2.4	3.0	0.8	2.6	5.2	0.9	1.2	2.0	0.7	1.2	1.0	0.8	2.2	3.6

5. CONCLUSION

Most elements in Es-16, Es-18, Es-14 and Es-17 showed good agreement with reference values. Quantification of the uncertainty due to inhomogeneity showed that the number of homogenous and moderately inhomogenous elements appeared higher in Es-17, Es-16 and Es-3 than in CAL-S. The concentrations of trace elements were higher in the candidate RM's than in CAL-S. More homogenous distribution and higher concentrations of Cs and Rb were found in Es-17, Es-3 and Es-16 than in MACS-3. Inhomogenous distribution of rare earth elements was observed in Es-14, Es-18 and Es-17 as elevated signals in ablation profiles due to enriched grains of unknown composition. Es-17 and Es-16 gave the best results with respect to the possible application as micro-analytical RM's.

Number of measurements greatly affects the resolution of homogeneity evaluation. Therefore more measurements should be performed for more reliable estimates. Pressed pellets of natural carbonate matrices are inferior to the synthetic carbonate MACS-3 as calibration RM's due to the inhomogenous distribution and lower concentrations of most elements but may serve as matrix matched quality control RM's for some elements.

The heterogeneities in the natural sedimentary limestone and dolomite samples may be on the same order of magnitude as ablation spot diameters and occur ubiquitously throughout the sample because compositional variations significantly larger than the uncertainty due to measurement procedure can be observed as evidenced by the homogeneity indices.

The uncertainty due to inhomogeneity for each analyte quantified as reliably as possible should be compared to the acceptance criterion and the homogeneity index should be checked as it provides important information about the ability to detect inhomogeneity. Therefore, analysis of the RSD's of inhomogeneity together with estimation of homogeneity indices is a suitable approach for evaluating homogeneity. For purposes of certifying an RM the preferable situation is when acceptance criterion is met and the inhomogeneity can be detected as it can then be quantified and included into the certified value thus providing a more complete characterization of the material. Outliers should always be examined in detail. Outlier analysis is useful for identifying groups of elements that are affected by inhomogeneity.

6. SUMMARY

Characterization of natural sedimentary dolomite and limestone reference materials from Geological Survey of Estonia using LA-ICP-MS

Martins Jansons

Sedimentary dolomite (Es-16, Es-18) and limestone (Es-3, Es-14, Es-17) from Geological Survey of Estonia have been used as reference materials in X-ray fluorescence analysis in Estonian laboratories. Homogeneity of these reference materials was investigated with laser-ablation inductively coupled plasma mass-spectrometry using MACS-3 and NIST 612 certified reference materials for calibration. Natural limestone CAL-S from CRPG was analyzed for overall comparison. For evaluating potential application of Es's as micro-analytical reference materials, different approaches, such as pairwise F-tests to MACS-3, estimation of homogeneity indices and quantification of uncertainty due to inhomogeneity were used. Estimation of homogeneity indices and analysis of uncertainties due to inhomogeneity together with statistical outlier analysis were found suitable for drawing conclusions about the true inhomogeneity of the samples. Most elements in Es-16, Es-18, Es-14 and Es-17 showed good agreement with reference values. Es-17 and Es-16 were found most homogenous with respect to the other samples. More homogenous distribution and higher concentrations of Cs and Rb were found in Es-17, Es-3 and Es-16 than in MACS-3. Inhomogenous distribution of rare earth elements was observed in Es-14, Es-18 and Es-17 as elevated signals in ablation profiles due to enriched grains of unknown composition.

7. KOKKUVÕTE

Looduslike Eesti Geoloogiateenistuse lubjakivi ja dolomiidi referentsmaterjalide mikroanalüüs kasutades LA-ICP-MS'i

Martinš Jansons

Eesti Geoloogiateenistuse poolt looduslike settekivimite baasil valmistatud dolomiidi (Es-16, Es-18) ja lubjakivi (Es-3, Es-14, Es-17) referentsmaterjale on röntgenfluoresentsanalüüsi kalibratisoonistandarditena kasutatud mitmetes Eesti laborites. Käesolevas töös kasutati nende materjalide homogeensuse hindamiseks ja mikrokarakteriseerimiseks laserablatsiooniga induktiivsidestatud plasma mass-spektromeetriat. Analüüsides kasutati kalibreerimiseks MACS-3 ja NIST 612 referentsmaterjalide ja võrdluseks analüüsiti CRPG CAL-S loodusliku lubjakivi standardit. Hindamaks Es-standardite sobivust mikroanalüütiliste referentsmaterjalidena kasutati F-testi MACS-3 standardi suhtes, homogeensuse indeksit ja proovi heterogeensusest põhjustatud määramatuse hinnangut. Kõige paremateks meetoditeks proovide tõelise homogeensuse hindamisel leiti olevat homogeensuse indeksid ja võõrväärtuste eemaldamisega teostatud heterogeensusest põhjustatud määramatuse hinnang. Es-16, Es-18, Es-14 ja Es-17 proovides olid enamike analüüsitud elementide sisaldused heas vastavuses referentsväärtustega. Kõigi analüüsitud proovide hulgast olid kõige homogeensemad Es-17 ja Es-16 standardid. Es-17, Es-3 ja Es-16 standardites olid Cs ja Rb homogeensema jaotuse ja kõrgema kontsentratsiooniga kui MACS-3 standardis. Määramata koostisega osakeste poolt põhjustatud haruldaste muldmetallide heterogeenset jaotumist ablatsiooniprofiilides täheldati standardites Es-14, Es-18 ja Es-17.

4. REFERENCES

[1] Y. Liu, Z. Hu, M. Li, and S. Gao, "Applications of LA-ICP-MS in the elemental analyses of geological samples," *Chinese Sci. Bull.*, vol. 58, no. 32, pp. 3863–3878, 2013.

[2] P. Richner, D. Evans, C. Wahrenberger, and V. Dietrich, "Applications of laser ablation and electrothermal vaporization as sample introduction techniques for ICP-MS," *Fresenius. J. Anal. Chem.*, vol. 350, no. 4–5, pp. 235–241, 1994.

[3] F. E. Cromwell and P. Arrowsmith, "Semiquantitative Analysis with Laser Ablation Inductively Coupled Plasma Mass Spectrometry," *Anal. Chem.*, vol. 67, no. 1, pp. 131–138, 1995.

[4] K. P. Jochum, D. Scholz, B. Stoll, U. Weis, S. A. Wilson, Q. Yang, A. Schwalb, N. Börner, D. E. Jacob, and M. O. Andreae, "Accurate trace element analysis of speleothems and biogenic calcium carbonates by LA-ICP-MS," *Chem. Geol.*, vol. 318–319, pp. 31–44, 2012.

[5] C. A. Heinrich, T. Pettke, W. E. Halter, M. Aigner-Torres, A. Audétat, D. Günther, B. Hattendorf, D. Bleiner, M. Guillong, and I. Horn, "Quantitative multi-element analysis of minerals, fluid and melt inclusions by laser-ablation inductively-coupled-plasma mass-spectrometry," *Geochim. Cosmochim. Acta*, vol. 67, no. 18, pp. 3473–3497, Sep. 2003.

[6] K. P. Jochum, U. Weis, B. Stoll, D. Kuzmin, Q. Yang, I. Raczek, D. E. Jacob, A. Stracke, K. Birbaum, D. a. Frick, D. Günther, and J. Enzweiler, "Determination of reference values for NIST SRM 610-617 glasses following ISO guidelines," *Geostand. Geoanalytical Res.*, vol. 35, pp. 397–429, 2011.

[7] T. Vaculovič, T. Warchilová, Z. Čadková, J. Száková, P. Tlustoš, V. Otruba, and V. Kanický, "Influence of laser ablation parameters on trueness of imaging," *Appl. Surf. Sci.*, vol. 351, pp. 296–302, 2015.

[8] M. E. Shaheen, J. E. Gagnon, and B. J. Fryer, "Femtosecond (fs) lasers coupled with modern ICP-MS instruments provide new and improved potential for in situ elemental and isotopic analyses in the geosciences," *Chem. Geol.*, vol. 330–331, pp. 260–273, 2012.

[9] N. L. LaHaye, S. S. Harilal, P. K. Diwakar, and A. Hassanein, "The effect of laser pulse duration on ICP-MS signal intensity, elemental fractionation, and detection limits in fs-LA-ICP-MS," *J. Anal. At. Spectrom.*, vol. 28, no. 11, p. 1781, 2013.

[10] I. Kroslakova and D. Günther, "Elemental fractionation in laser ablation-inductively coupled plasma-mass spectrometry: evidence for mass load induced matrix effects in the ICP during ablation of a silicate glass," *J. Anal. At. Spectrom.*, vol. 22, no. 1, pp. 51–62, 2007.

[11] C. D'Oriano, S. Da Pelo, F. Podda, and R. Cioni, "Laser-ablation inductively coupled plasma mass spectrometry (LA-ICP-MS): Setting operating conditions and instrumental performance," *Period. di Mineral.*, vol. 77, no. 3, pp. 65–74, 2008.

[12] P. K. Diwakar, J. J. Gonzalez, S. S. Harilal, R. E. Russo, and A. Hassanein, "Ultrafast laser ablation ICP-MS: role of spot size, laser fluence, and repetition rate in signal intensity and elemental fractionation," *J. Anal. At. Spectrom.*, vol. 29, no. 207890, p. 339, 2014.

[13] D. Beauchemin, “Inductively Coupled Plasma Mass Spectrometry,” *Anal. Chem.*, vol. 78, no. 12, pp. 4111–4136, Jun. 2006.

[14] D. Günther and B. Hattendorf, “Solid sample analysis using laser ablation inductively coupled plasma mass spectrometry,” *TrAC Trends Anal. Chem.*, vol. 24, no. 3, pp. 255–265, Mar. 2005.

[15] J. L. Fernández-Turiel, J. F. Llorens, F. López-Vera, C. Gómez-Artola, I. Morell, and D. Gimeno, “Strategy for water analysis using ICP-MS,” *Fresenius. J. Anal. Chem.*, vol. 368, no. 6, pp. 601–606, Nov. 2000.

[16] D. Potter, “A commercial perspective on the growth and development of the quadrupole ICP-MS market,” *J. Anal. At. Spectrom.*, vol. 23, no. 5, p. 690, 2008.

[17] R. E. Russo, X. Mao, J. J. Gonzalez, V. Zorba, and J. Yoo, “Laser Ablation in Analytical Chemistry,” *Anal. Chem.*, vol. 85, no. 13, pp. 6162–6177, Jul. 2013.

[18] A. Charriau, S. Lissalde, G. Poulier, N. Mazzella, R. Buzier, and G. Guibaud, “Overview of the Chemcatcher® for the passive sampling of various pollutants in aquatic environments Part A: Principles, calibration, preparation and analysis of the sampler,” *Talanta*, vol. 148, pp. 556–571, 2015.

[19] L. Björklund Blom, G. M. Morrison, J. Kingston, G. A. Mills, R. Greenwood, T. J. R. Pettersson, and S. Rauch, “Performance of an in situ passive sampling system for metals in stormwater,” *J. Environ. Monit.*, vol. 4, no. 2, pp. 258–262, Mar. 2002.

[20] J. S. Becker, A. Matusch, and B. Wu, “Bioimaging mass spectrometry of trace elements - recent advance and applications of LA-ICP-MS: A review,” *Anal. Chim. Acta*, vol. 835, pp. 1–18, 2014.

[21] A. V. Lazartigues, P. Sirois, and D. Savard, “LA-ICP-MS analysis of small samples: Carbonate reference materials and larval fish otoliths,” *Geostand. Geoanalytical Res.*, vol. 38, pp. 225–240, 2014.

[22] S. J. Batenburg, G. J. Reichart, T. Jilbert, M. Janse, F. P. Wesselingh, and W. Renema, “Interannual climate variability in the Miocene: High resolution trace element and stable isotope ratios in giant clams,” *Palaeogeogr. Palaeoclimatol. Palaeoecol.*, vol. 306, no. 1–2, pp. 75–81, 2011.

[23] S. J. Fallon, M. T. McCulloch, R. Van Woesik, and D. J. Sinclair, “Corals at their latitudinal limits: Laser ablation trace element systematics in Porites from Shirigai Bay, Japan,” *Earth Planet. Sci. Lett.*, vol. 172, no. 3–4, pp. 221–238, 1999.

[24] N. Miliszkiewicz, S. Walas, and A. Tobiasz, “Current approaches to calibration of LA-ICP-MS analysis,” *J. Anal. At. Spectrom.*, vol. 30, pp. 327–338, 2015.

[25] P. Basnet, D. Amarasiriwardena, F. Wu, Z. Fu, and T. Zhang, “Elemental bioimaging of tissue level trace metal distributions in rice seeds (Oryza sativa L.) from a mining area in China.,” *Environ. Pollut.*, vol. 195C, pp. 148–156, 2014.

[26] A. Hanć, A. Piechalak, B. Tomaszewska, and D. Barałkiewicz, “Laser ablation inductively coupled plasma mass spectrometry in quantitative analysis and imaging of plant’s thin sections,” *Int. J. Mass Spectrom.*, vol. 363, no. 1, pp. 16–22, 2014.

[27] S. F. L. Watt, D. M. Pyle, T. A. Mather, J. A. Day, and A. Aiuppa, “The use of tree-rings and foliage as an archive of volcanogenic cation deposition,” *Environ. Pollut.*, vol. 148, no. 1, pp. 48–61, Jul. 2007.

[28] M. Noël, J. R. Christensen, J. Spence, and C. T. Robbins, “Using laser ablation inductively coupled plasma mass spectrometry (LA-ICP-MS) to characterize copper, zinc and mercury along grizzly bear hair providing estimate of diet.,” *Sci. Total Environ.*, vol. 529, pp. 1–9, 2015.

[29] F. A. Orellana, C. G. Gálvez, F. A. Orellana, C. G. Gálvez, M. T. Roldán, C. García-Ruiz, M. T. Roldán, and C. García-Ruiz, “Applications of laser-ablation-inductively-coupled plasma-mass spectrometry in chemical analysis of forensic evidence,” *TrAC Trends Anal. Chem.*, vol. 42, pp. 1–34, 2013.

[30] J. S. Becker and D. Salber, “New mass spectrometric tools in brain research,” *TrAC Trends Anal. Chem.*, vol. 29, no. 9, pp. 966–979, 2010.

[31] J. S. Becker, “Bioimaging of metals in brain tissue from micrometre to nanometre scale by laser ablation inductively coupled plasma mass spectrometry: State of the art and perspectives,” *Int. J. Mass Spectrom.*, vol. 289, no. 2–3, pp. 65–75, 2010.

[32] W. N. Tzeng, C. W. Chang, C. H. Wang, J. C. Shiao, Y. Iizuka, Y. J. Yang, C. F. You, and L. Lozys, “Misidentification of the migratory history of anguillid eels by Sr/Ca ratios of vaterite otoliths,” *Mar. Ecol. Ser.*, vol. 348, pp. 285–295, 2007.

[33] T. Pettke, F. Oberli, A. Audétat, M. Guillong, A. C. Simon, J. J. Hanley, and L. M. Klemm, “Recent developments in element concentration and isotope ratio analysis of individual fluid inclusions by laser ablation single and multiple collector ICP-MS,” *Ore Geol. Rev.*, vol. 44, pp. 10–38, 2012.

[34] V. Rudovica, A. Viksna, and A. Actins, “Application of LA-ICP-MS as a rapid tool for analysis of elemental impurities in active pharmaceutical ingredients,” *J. Pharm. Biomed. Anal.*, vol. 91, pp. 119–122, 2014.

[35] J. J. Leach, L. a Allen, D. B. Aeschliman, and R. S. Houk, “Calibration of laser ablation inductively coupled plasma mass spectrometry using standard additions with dried solution aerosols,” *Anal. Chem.*, vol. 71, no. 2, pp. 440–445, 1999.

[36] H. P. Longerich, S. E. Jackson, and D. Gunther, “Inter-laboratory note. Laser ablation inductively coupled plasma mass spectrometric transient signal data acquisition and analyte concentration calculation,” *J. Anal. At. Spectrom.*, vol. 11, no. 9, pp. 899–904, 1996.

[37] International Organization for Standardization, “Certification of reference materials — General and statistical principles,” *ISO Guide 35:1989*. Geneva, Switzerland, p. 32, 1989.

[38] J. S. Kane, P. J. Potts, T. Meisel, and M. Wiedenbeck, “International association of geoanalysts’ protocol for the certification of geological and environmental reference materials: A supplement,” *Geostand. Geoanalytical Res.*, vol. 31, pp. 285–288, 2007.

[39] J. Pauwels, A. Lamberty, and H. Schimmel, “Homogeneity testing of reference materials,” *Accredit. Qual. Assur.*, vol. 3, no. 2, pp. 51–55, Feb. 1998.

[40] M. Guillong, K. Hametner, E. Reusser, S. A. Wilson, and D. Günther, “Preliminary characterisation of new glass reference materials (GSA-1G, GSC-1G, GSD-1G and GSE-1G) by laser ablation-inductively coupled plasma-mass spectrometry using 193 nm, 213 nm and 266 nm wavelengths,” *Geostand. Geoanalytical Res.*, vol. 29, no. 3, pp. 315–331, 2005.

[41] U.S. Geological Survey, “Geochemical Reference Materials and Certificates: New Reference Materials In Production.” [Online]. Available: http://crustal.usgs.gov/geochemical_reference_standards/RM_development.html. [Accessed: 31-Jan-2016].

[42] S. A. Wilson, A. E. Koening, and R. Orklid, “Development of microanalytical reference material (MACS-3) for LA-ICP-MS analysis of carbonate samples,” in *Goldschmidt Conference Abstracts*, 2008, p. 1025.

[43] J. Pauwels, A. Lamberty, and H. Schimmel, “Homogeneity testing of reference materials,” *Accredit. Qual. Assur.*, vol. 3, no. 2, pp. 51–55, 1998.

[44] D. Harries, “Homogeneity testing of microanalytical reference materials by electron probe microanalysis (EPMA),” *Chemie der Erde - Geochemistry*, vol. 74, no. 3, pp. 375–384, 2014.

[45] B. J. Fryer, S. E. Jackson, and H. P. Longerich, “The application of laser ablation microprobe-inductively coupled plasma-mass spectrometry (LAM-ICP-MS) to in situ (U)-Pb geochronology,” *Chem. Geol.*, vol. 109, no. 1–4, pp. 1–8, Oct. 1993.

[46] E. Jarosewich and L. A. Boatner, “Rare-Earth Element Reference Samples for Electron Microprobe Analysis,” *Geostand. Geoanalytical Res.*, vol. 15, no. 2, pp. 397–399, Oct. 1991.

[47] J. B. Hunt and P. G. Hill, “An inter-laboratory comparison of the electron probe microanalysis of glass geochemistry,” *Quat. Int.*, vol. 34–36, no. 95, pp. 229–241, Jan. 1996.

[48] M. L. Patino-Douce, A. Patino-Douce, M. Qayyum, and R. L. Nielsen, “New set of low concentration standards for La, Ce, Sm, Yb, Lu, Y, Sc, V, Nb and Ta in silicates,” *Geostand. Geoanalytical Res.*, vol. 18, no. 2, pp. 195–198, Oct. 1994.

[49] T. Kiipli, R. A. Batchelor, J. P. Bernal, and C. Cowing, “Seven sedimentary rock reference samples from Estonia,” *Oil Shale*, vol. 17, no. 3, pp. 215–223, 2000.

[50] P. J. Potts, M. Thompson, J. S. Kane, P. C. Webb, and J. Carigan, “GEOPT6 - An international proficiency test for analytical geochemistry laboratories - Report on round 6 (OU-3: Nanhorn microgranite) and 6A (CAL-S: CRPG limestone).” International Association of Geoanalysts, p. 52, 2000.

[51] L. Chen, Y. Liu, Z. Hu, S. Gao, K. Zong, and H. Chen, “Accurate determinations of fifty-four major and trace elements in carbonate by LA-ICP-MS using normalization strategy of bulk components as 100%,” *Chem. Geol.*, vol. 284, no. 3–4, pp. 283–295, 2011.

[52] A. Williams and S. L. R. Ellison, “Eurachem/CITAC Guide: Quantifying Uncertainty in Analytical Measurement, (3rd ed. 2012).,” 2012. [Online]. Available: www.eurachem.org.

5. APPENDICES

Appendix 1

Table 8.1. Relative $u_{inhom.}$ at each spot diameter for NIST 612, MACS-3 and CAL-S.

	NIST 612			MACS-3			CAL-S		
	40 µm	65 µm	100 µm	40 µm	65 µm	100 µm	40 µm	65 µm	100 µm
Na	5.4%	3.2%	2.1%	9.8%	3.1%	2.5%	26.8%	15.4%	15.4%
P	N/A	17.5%	14.6%	71.7%	0.5%	8.7%	N/A	27.7%	26.5%
Ca	7.9%	2.2%	1.7%	7.1%	3.7%	2.3%	12.3%	5.4%	3.3%
Sc	4.0%	2.4%	4.5%	7.1%	2.9%	2.2%	N/A	N/A	21.6%
Ti	8.0%	6.7%	8.5%	9.8%	5.5%	4.8%	34.1%	36.7%	36.5%
V	7.7%	9.7%	3.2%	10.4%	3.7%	3.1%	22.6%	15.8%	5.4%
Cr	9.6%	11.7%	7.3%	7.9%	5.2%	3.2%	28.5%	20.6%	8.5%
Mn	8.1%	2.9%	3.4%	11.6%	5.6%	2.0%	15.2%	5.1%	3.2%
Co	6.0%	3.7%	2.7%	9.3%	2.6%	2.6%	123.3%	41.3%	25.8%
Ni	8.9%	5.9%	3.4%	8.2%	3.7%	2.9%	76.3%	45.2%	41.5%
Cu	7.3%	2.4%	1.8%	9.5%	4.0%	2.3%	50.0%	38.4%	18.2%
Zn	9.8%	5.7%	5.0%	8.6%	4.0%	2.3%	31.9%	11.5%	9.4%
Ga	6.6%	7.9%	4.5%	9.6%	4.2%	3.8%	26.3%	32.0%	74.2%
Rb	3.6%	2.3%	1.4%	34.2%	19.5%	140.7%	242.4%	36.4%	25.0%
Sr	7.5%	2.9%	1.4%	9.5%	4.3%	3.1%	14.5%	4.4%	3.8%
Y	3.8%	4.5%	3.3%	8.0%	2.9%	2.9%	8.7%	5.3%	4.0%
Zr	7.3%	3.6%	1.8%	7.8%	2.3%	2.6%	46.4%	28.0%	50.0%
Nb	10.9%	6.2%	3.3%	9.4%	2.9%	3.0%	36.1%	32.0%	22.6%
Mo	11.0%	6.4%	3.9%	13.8%	6.9%	5.1%	39.6%	28.5%	15.7%
Ag	7.0%	9.1%	4.1%	10.9%	4.6%	5.2%	N/A	N/A	N/A
Cd	9.3%	5.1%	3.1%	9.4%	3.9%	2.8%	11.7%	29.8%	14.2%
Sn	10.1%	9.2%	2.6%	8.1%	3.2%	2.9%	24.0%	95.2%	55.2%
Sb	13.6%	9.5%	5.1%	7.9%	4.3%	2.5%	73.7%	32.1%	28.3%
Cs	6.1%	2.9%	0.9%	N/A	57.0%	26.1%	N/A	N/A	N/A
Ba	7.3%	5.2%	3.3%	8.1%	4.8%	3.0%	24.3%	15.7%	16.9%
La	6.4%	2.7%	2.3%	7.4%	3.7%	2.1%	7.0%	6.2%	3.7%
Ce	4.6%	3.8%	2.2%	10.0%	3.4%	2.5%	28.9%	38.5%	7.9%
Pr	7.7%	3.8%	3.6%	8.8%	3.9%	2.3%	15.6%	16.6%	13.7%
Nd	4.2%	2.9%	2.4%	10.0%	3.8%	2.5%	14.8%	15.6%	6.3%
Sm	3.8%	2.9%	3.2%	5.6%	4.0%	2.1%	41.0%	19.6%	23.8%
Eu	4.4%	3.9%	2.1%	8.1%	3.8%	1.8%	51.4%	30.7%	37.8%
Gd	4.9%	3.6%	2.2%	8.0%	3.3%	3.2%	37.7%	18.5%	20.2%
Tb	4.5%	3.2%	2.5%	7.0%	4.1%	2.2%	49.6%	16.4%	24.0%
Dy	2.4%	4.5%	2.7%	8.3%	3.7%	2.6%	39.8%	20.4%	9.8%
Ho	7.0%	3.8%	3.6%	6.2%	3.3%	2.4%	27.4%	17.5%	6.8%
Er	4.1%	4.4%	3.3%	7.2%	3.6%	2.9%	33.9%	17.4%	10.3%
Tm	4.3%	3.9%	2.9%	7.7%	3.1%	2.0%	36.0%	27.3%	11.2%
Yb	5.6%	3.7%	3.2%	7.4%	3.6%	2.6%	41.1%	12.1%	11.4%
Lu	4.5%	4.3%	3.2%	5.7%	3.9%	2.4%	33.3%	22.2%	15.2%
Hf	8.2%	5.3%	2.4%	7.2%	3.3%	2.5%	54.8%	61.2%	49.1%
Ta	2.2%	5.9%	1.9%	9.3%	3.4%	2.7%	61.3%	72.7%	67.7%
Pb	6.7%	7.7%	2.7%	11.2%	3.5%	4.7%	34.1%	39.3%	38.2%
Bi	9.0%	13.1%	3.9%	11.0%	4.9%	5.0%	N/A	42.8%	56.2%
Th	3.3%	3.2%	3.3%	7.4%	3.0%	1.9%	48.0%	30.4%	27.5%
U	2.3%	4.5%	3.1%	17.6%	11.5%	7.1%	10.3%	5.9%	0.5%

Table 8.2. Relative $u_{inhom.}$ at each spot diameter for Es-14, Es-18 and Es-3.

	Es-14			Es-18			Es-3		
	40 µm	65 µm	100 µm	40 µm	65 µm	100 µm	40 µm	65 µm	100 µm
Na	10.4%	9.5%	10.9%	67.2%	13.2%	19.5%	55.4%	16.3%	38.3%
P	25.6%	16.8%	7.1%	93.0%	17.1%	3.6%	18.0%	11.2%	8.2%
Ca	3.8%	2.4%	1.3%	3.9%	2.5%	0.4%	4.2%	0.9%	0.9%
Sc	15.2%	7.6%	5.2%	19.7%	42.6%	13.7%	15.7%	8.6%	3.2%
Ti	40.8%	27.7%	52.5%	44.7%	67.0%	31.4%	30.0%	54.6%	9.6%
V	8.6%	11.5%	6.1%	3.3%	5.1%	2.9%	10.5%	8.7%	7.1%
Cr	127.6%	62.2%	25.2%	16.7%	6.4%	138.1%	15.2%	4.9%	6.4%
Mn	19.3%	8.7%	6.9%	12.9%	1.6%	4.4%	21.3%	5.0%	10.4%
Co	43.7%	21.6%	11.8%	16.4%	16.0%	8.8%	14.6%	15.1%	24.1%
Ni	34.5%	63.7%	16.1%	6.1%	20.6%	23.7%	21.3%	44.2%	7.6%
Cu	25.9%	89.5%	10.7%	28.5%	35.1%	47.5%	61.7%	13.4%	13.8%
Zn	44.9%	21.1%	81.6%	20.1%	7.7%	8.6%	26.8%	18.2%	20.2%
Ga	8.3%	7.3%	6.4%	22.9%	10.1%	15.4%	12.9%	6.1%	6.9%
Rb	13.5%	4.6%	8.3%	36.2%	10.8%	25.6%	13.6%	7.7%	7.7%
Sr	6.1%	3.8%	4.2%	4.6%	0.6%	3.5%	34.9%	4.5%	3.6%
Y	11.0%	28.2%	11.4%	13.4%	37.6%	25.3%	27.7%	23.7%	9.4%
Zr	27.6%	59.8%	59.5%	27.6%	31.5%	108.1%	20.3%	14.6%	33.2%
Nb	40.8%	19.6%	54.9%	25.4%	19.2%	26.0%	40.8%	30.7%	46.2%
Mo	30.3%	47.5%	22.5%	21.6%	98.4%	22.5%	33.0%	39.0%	33.7%
Ag	60.1%	90.4%	62.7%	N/A	N/A	N/A	N/A	N/A	N/A
Cd	120.2%	86.7%	15.8%	N/A	N/A	27.7%	N/A	14.5%	N/A
Sn	54.1%	17.4%	36.7%	34.7%	20.2%	9.3%	25.3%	18.6%	29.9%
Sb	24.0%	27.9%	78.1%	N/A	26.8%	60.0%	33.5%	62.2%	31.6%
Cs	46.1%	9.5%	7.8%	27.3%	6.9%	9.8%	18.8%	11.1%	8.2%
Ba	26.4%	53.3%	31.3%	87.0%	58.4%	50.2%	58.0%	10.1%	29.7%
La	8.3%	13.1%	4.9%	35.3%	55.7%	112.7%	7.3%	5.6%	9.4%
Ce	9.6%	10.5%	5.2%	26.7%	52.3%	24.3%	31.0%	25.7%	24.0%
Pr	99.4%	10.6%	4.3%	38.2%	11.6%	18.0%	7.9%	6.3%	10.0%
Nd	30.7%	19.4%	10.2%	39.9%	40.3%	29.7%	5.8%	6.6%	9.9%
Sm	23.6%	16.0%	2.9%	35.6%	30.1%	14.4%	12.2%	7.3%	8.8%
Eu	8.0%	14.6%	2.6%	55.3%	19.1%	65.1%	7.5%	12.8%	15.5%
Gd	12.9%	24.1%	7.6%	19.7%	16.3%	77.6%	24.2%	25.7%	38.4%
Tb	19.7%	30.9%	6.7%	17.1%	17.5%	5.7%	22.6%	10.6%	9.4%
Dy	11.0%	11.1%	8.4%	11.2%	24.4%	7.5%	17.9%	10.9%	8.1%
Ho	17.1%	27.2%	10.3%	6.1%	39.0%	31.8%	14.6%	9.9%	6.7%
Er	13.2%	46.9%	14.1%	4.5%	13.2%	19.9%	20.1%	13.2%	6.0%
Tm	15.2%	28.0%	15.6%	20.0%	70.9%	39.4%	27.7%	13.4%	13.2%
Yb	11.5%	30.5%	17.6%	23.2%	10.1%	24.5%	15.4%	11.9%	10.5%
Lu	17.5%	28.2%	24.2%	20.5%	122.1%	42.4%	20.1%	10.7%	11.9%
Hf	22.4%	73.1%	81.9%	47.0%	48.5%	31.0%	11.5%	19.4%	16.4%
Ta	38.0%	24.1%	70.4%	33.5%	18.5%	22.4%	46.4%	28.2%	23.8%
Pb	93.1%	37.0%	30.3%	47.1%	25.6%	75.9%	38.1%	48.3%	29.1%
Bi	75.9%	60.2%	64.8%	39.2%	60.1%	50.3%	79.2%	33.0%	15.9%
Th	87.3%	15.6%	11.1%	13.2%	57.6%	12.7%	5.9%	14.2%	6.9%
U	15.1%	21.5%	11.8%	17.8%	33.5%	32.2%	13.7%	3.8%	11.5%

Table 8.3. Relative $u_{inhom.}$ at each spot diameter for Es-17 and Es-16.

	Es-17			Es-16		
	40 µm	65 µm	100 µm	40 µm	65 µm	100 µm
Na	18.0%	24.0%	6.5%	268.4%	34.3%	5.9%
P	N/A	7.2%	19.5%	33.8%	8.1%	4.6%
Ca	5.9%	2.1%	1.4%	5.8%	1.1%	1.6%
Sc	9.8%	5.2%	4.6%	21.0%	5.0%	1.8%
Ti	7.5%	16.2%	14.9%	11.2%	26.2%	24.0%
V	11.0%	3.6%	2.4%	14.1%	3.0%	4.9%
Cr	13.1%	6.0%	5.5%	16.2%	11.4%	36.9%
Mn	8.2%	10.8%	7.2%	6.1%	2.8%	3.0%
Co	20.0%	3.4%	5.6%	22.9%	12.1%	9.7%
Ni	27.2%	8.9%	12.8%	30.8%	10.8%	14.4%
Cu	61.5%	17.9%	36.9%	56.4%	58.3%	18.6%
Zn	19.5%	5.5%	8.2%	14.0%	13.1%	96.1%
Ga	15.0%	6.0%	2.6%	13.8%	4.6%	2.9%
Rb	10.7%	9.7%	4.0%	9.6%	9.9%	4.7%
Sr	6.0%	4.3%	5.1%	52.2%	3.3%	1.2%
Y	5.4%	35.2%	2.9%	9.7%	5.3%	4.5%
Zr	14.5%	25.8%	21.1%	19.9%	18.8%	31.0%
Nb	24.2%	20.0%	5.8%	19.6%	22.0%	20.9%
Mo	154.5%	44.7%	90.2%	55.5%	21.8%	15.7%
Ag	N/A	N/A	N/A	N/A	N/A	N/A
Cd	N/A	N/A	35.8%	N/A	N/A	N/A
Sn	36.4%	10.1%	6.8%	38.2%	13.3%	17.0%
Sb	N/A	30.9%	109.5%	26.0%	18.3%	13.4%
Cs	13.7%	16.0%	6.1%	17.1%	8.1%	7.9%
Ba	22.5%	32.1%	15.8%	20.6%	11.1%	11.6%
La	9.8%	4.8%	4.3%	8.0%	5.8%	3.2%
Ce	41.7%	11.5%	14.9%	48.3%	29.9%	26.0%
Pr	7.9%	7.7%	5.0%	9.7%	7.7%	4.2%
Nd	4.8%	4.6%	3.3%	12.6%	8.3%	3.4%
Sm	10.9%	6.2%	5.2%	12.6%	9.2%	7.3%
Eu	8.0%	9.4%	5.8%	18.9%	9.0%	6.6%
Gd	28.8%	34.6%	35.9%	22.4%	26.1%	19.3%
Tb	7.2%	28.3%	5.9%	9.5%	9.7%	6.4%
Dy	3.7%	41.8%	5.5%	14.1%	3.9%	4.0%
Ho	15.0%	39.7%	5.4%	10.1%	6.1%	3.5%
Er	11.3%	36.1%	5.2%	4.0%	6.7%	4.1%
Tm	19.0%	39.2%	6.7%	12.7%	7.7%	4.9%
Yb	4.0%	3.3%	10.1%	13.3%	4.2%	1.8%
Lu	8.6%	25.3%	11.6%	13.3%	7.2%	1.8%
Hf	14.9%	20.2%	17.1%	16.1%	10.9%	24.8%
Ta	17.7%	15.8%	32.5%	30.9%	18.7%	34.5%
Pb	81.3%	24.1%	21.1%	86.6%	32.3%	14.4%
Bi	N/A	29.5%	17.9%	56.2%	38.1%	18.0%
Th	6.9%	3.7%	4.3%	16.5%	15.7%	6.9%
U	10.5%	3.0%	1.5%	10.8%	10.0%	13.1%

Table 8.4. Cases with more than two times the average number of outliers occurring together. Values shaded in grey deviate by more than 2 standard deviations from the median.

	40 µm spot diameter							65 µm square spot							100 µm spot diameter									
	CAL-S	MACS-3	MACS-3	Es-14	Es-16	Es-18	Es-18	MACS-3	Es-14	Es-14	Es-16	Es-17	Es-18	Es-18	CAL-S	CAL-S	MACS-3	MACS-3	NIST 612	Es-14	Es-14	Es-17	Es-18	Es-18	Es-3
Na	2E+02	7E+03	7E+03	3E+02	1E+04	3E+02	7E+02	6E+03	3E+02	3E+02	3E+02	2E+02	2E+02	3E+02	1E+02	1E+02	6E+03	5E+03	1E+05	2E+02	2E+02	2E+02	3E+02	2E+02	6E+02
P			6066	113.2	1017	1633	3050	120.5	135.1	114.7	1761	38.8	176.4	240.5	29.1	32	255	135.2	57.8	76.5	73.8	40.9	226.5	220	2352
Ca	3E+05	5E+05	4E+05	3E+05	3E+05	2E+05	2E+05	4E+05	3E+05	3E+05	2E+05	3E+05	2E+05	2E+05	4E+05	4E+05	4E+05	4E+05	9E+04	3E+05	3E+05	3E+05	2E+05	2E+05	4E+05
Sc		24.3	21.9	2.4	2.3	1.5	1	24.9	2.3	2.3	2.3	1.8	3.6	1.5	0.2	0.1	21.2	24.4	41.5	2.1	2.3	2.1	2	1.4	2.5
Ti	108.1	75.6	70.1	1144	399.7	683.4	252.1	68.5	657.3	991.1	547.9	844.8	281.3	294.3	37.2	10.3	78.9	63	46.4	1795	1032	558.9	675.4	278	612.7
V	5	62.7	65.5	11.8	9	22.6	16.7	53.9	14	15.9	9	9.6	19.4	17.6	1.8	2.9	49.9	46.5	38.7	11.5	13.8	9.5	19.1	17.9	7.8
Cr	6.9	167.4	180.4	22.9	8.1	10.1	7.5	143.6	75.2	25.5	10.2	9.1	9.6	9.5	4.2	4.2	199	131.6	40.4	29.8	28.1	8.8	9.1	9.4	8.7
Mn	18.9	564.8	653.2	117.1	2161	433.3	337.2	548.6	116.9	133.8	2028	225.2	429.4	394.2	9.7	9.1	512.8	508.8	37.6	102.5	110.4	233.3	381.2	379.2	414.9
Co	0.9	74.9	67	2.9	1	1.1	0.7	54.5	2.9	4.4	0.8	1.3	0.7	0.7	0.1	0.1	51.7	50.8	36.2	2.3	2.6	1.4	0.7	0.7	0.9
Ni	1.7	91.5	67.5	8.2	4.7	1.4	2.3	54.3	8.9	32.9	2.8	3.6	2.1	2.1	3.7	5.4	61.4	53.5	39.3	7.2	8.8	4.9	2	1.9	4.1
Cu	2.3	115.6	98.2	10	0.7	1.5		119.1	10.9	12.1	1.4	1.3	0.6	0.6	1.3	1.1	94.1	103.7	39.9	8.7	11.6	2.8	0.6	0.6	1.6
Zn	8	127.4	142.4	9.9	8.2	8.4	7.6	125.1	271.6	14.4	9.4	8.1	6.2	6.9	11.7	58.4	119.1	113.5	37.7	11.9	13.3	8.8	7.3	6.9	5.5
Ga	0.2	24.7	21.4	3.1	8.1	2.8	1.7	18.1	2.9	3	2	2.4	1.4	1.7	0.1	0.1	18.2	16.4	37.2	2.4	2.6	2.6	2.1	1.9	1.7
Rb	12			16.2	13.9	25	11.6	0.1	18.1	18	13	14.7	9.8	13.2	0.7	0.1	0.7		31.6	15.4	15.1	15.6	20.8	12.1	11.0
Sr	208.7	9157	7826	554.6	183.2	56.3	46.3	6664	538.9	543.7	63.5	123.2	52.5	49.6	201.3	214.8	7031	6616	78.5	508.1	507.9	131.5	51.8	51.2	314
Y	2	23.8	24.4	6.9	11.1	5.7	4.4	25.9	11.8	7.3	15.4	17.4	13	5.7	1.8	1.8	22.3	26.1	39	8.9	7.1	8.3	6.1	10.8	13.9
Zr	2.2	10.4	11.3	11.9	7.6	13.9	7	9.8	15	18.2	10.3	13.6	2095	9.2	0.9	0.7	10.3	9.4	36.6	48.7	13.6	15	70.3	11.8	11.7
Nb	0.2	57.5	72.7	3	0.8	1.2	0.6	56	3.1	3.8	1.2	2.9	0.9	0.9	0.1	0.1	60.1	55.6	37.7	6.7	9.1	1.8	1.8	0.8	3.6
Mo	0.1	1.8	2	0.6	0.1	0.1	0.1	1.6	0.7	0.9	0.1	0.3	0.1	0.1	0.2	0.7	1.5	1.3	39.3	0.7	0.9	0.7	0.1	0	0.4
Ag		88.2	82	5.6				61.9	2.3	11.3			0.1				67.5	57.3	22.1	1.7	2.6		0		
Cd		66.7	62.9	41.1				61.5	6.3	14.2				0.1	0.3	0.3	58.4	57.3	29.6	4.3	6.4	0	0.1	0.1	0.1
Sn		75.9	69.7	33	0.4	0.5	0.2	60.7	17	21.9	0.4	0.3	0.3	0.2	0.4	0.1	60.4	53.1	38.8	15.1	14.5	0.3	0.2	0.2	0.3
Sb		36.3	43.1	5.4		0.1		28.6	8.8	11.5	0.1		0.1	0	0.2	0.2	32.7	24.6	38.5	6.6	7	0.1	0.1	0	0.2
Cs	1.7			0.7	1	0.7	0.3	0	0.9	0.9	0.7	0.6	0.5	0.5	0		0		42.2	0.7	0.7	0.6	0.5	0.5	0.7
Ba	19.8	74.5	65.4	160.2	46.7	99.2	29.2	60.2	122.6	128	37.3	36.4	21.2	27.4	8.5	1.4	64	55.6	39.1	190.9	243.1	38.1	76.9	44	28.4
La	1.8	13.6	13.5	811.4	9.1	7	13.1	11.8	6.9	8.5	11.9	13.7	6.5	16.7	0.9	0.9	11.4	11.1	37.4	6.5	6.8	14.7	11.7	41.8	9.0
Ce	2.2	14.1	17.1	12.4	28.8	14.1	23.1	11.3	12.5	13.7	21.2	32.9	12	30.5	0.5	0.4	11.7	10.9	39	10.9	11.6	25.5	17.9	72.5	38.1
Pr	0.3	13.8	13.5	8.5	2.2	1.5	3.2	12.9	1.5	1.8	2.9	2.7	1.6	3.5	0.1	0.1	11.2	11.6	38.2	1.5	1.5	2.7	1.9	8.8	2.1
Nd	1.5	12.1	12.4	12.5	9.6	5.4	12.2	12	6.7	7.5	12.5	10.5	5.8	12.5	0.4	0.4	11.2	11	36.5	6.3	8	10.4	10	34.6	8.8
Sm	0.3	11.5	12.6	1.4	2.3	1.1	2.4	12.4	1.4	1.4	3	1.9	1.3	2.2	0.1	0.1	10.2	11.2	37.8	1.2	1.2	1.9	1.4	6.1	2.1
Eu	0.1	13.4	12.6	0.3	0.8	0.8	0.4	12.1	0.3	0.3	0.6	0.5	0.3	0.4	0	0	10.9	10.9	35.8	0.3	0.3	0.4	0.4	0.9	0.5
Gd	0.2	11.5	11.7	1.3	4.4	1.1	1.8	12.2	2	1.3	3.4	3.5	1.4	1.6	0.1	0.1	10.4	10.8	37.6	1.4	1.2	1.9	1.3	5	8.8
Tb	0	11.1	10.3	0.2	0.3	0.2	0.2	11.9	0.3	0.2	0.4	0.4	0.2	0.2	0	0	10.4	11	36.9	0.2	0.2	0.2	0.2	0.6	0.4
Dy	0.2	12.4	13	1.2	1.5	1	1.1	12.1	2.3	1.2	2.4	3.1	1.7	1.1	0.1	0.1	10.9	11.6	37.2	1.3	1.2	1.3	1.1	2.6	2.1
Ho	0.1	12	13.6	0.2	0.4	0.2	0.2	12.9	0.4	0.2	0.5	0.6	0.4	0.2	0	0	10.7	12	38.5	0.3	0.2	0.3	0.2	0.4	0.5
Er	0.1	13.5	13.2	0.7	1	0.5	0.5	12.9	1.4	0.6	1.2	1.4	1.6	0.6	0.1	0.1	10.9	12.2	39	0.8	0.7	0.6	0.5	0.8	1.2
Tm	0	14.8	11.5	0.1	0.2	0.1	0	13.3	0.1	0.1	0.2	0.2	0.3	0.1	0	0	11.7	13	38.4	0.1	0.1	0.1	0.1	0.1	0.3
Yb	0.2	13.6	14.5	0.6	0.7	0.4	0.4	13.9	0.9	0.7	1	1.1	2.3	0.4	0.1	0.1	11.5	12.9	41	0.8	0.6	0.5	0.6	0.5	0.9
Lu	0	13.3	12.5	0.1	0.1	0.1		13.5	0.1	0.1	0.1	0.1	0.5	0.1	0	0	11	12.2	39	0.1	0.1	0.1	0.1	0.1	0.2
Hf	0.1	5.9	6.4	0.3	0.3	0.6	0.3	5.6	0.4	0.5	0.3	0.5	40.9	0.2	0	0	5.3	5.7	35.8	2.1	0.4	0.5	0.7	0.4	0.4
Ta		29.3	28.2	0.1	0.1	0.1	0.1	27	0.1	0.2	0.1	0.2	0.1	0.1	0	0	25.6	26.5	40.9	0.4	0.5	0.1	0.1	0.1	0.2
Pb	1.3	91.2	104.9	654.1	8.4	2.4	1.2	64.9	194.9	214.5	1.5	3.7	0.7	0.8	2.4	1.8	71.5	61.9	40	168.8	103.7	4.9	3.3	2.2	3.6
Bi		27.5	31.4	28.2	0.1	0.1		22.2	14.4	27.1	0	0	0	0	0.2		24.4	21.1	29.8	32	48.1	0	0	0	0.1
Th	0.3	66	61.4	6.7	2.6	1.6	1.2	63.9	1.7	1.8	3.4	3.5	1.9	3.8	0.1	0	54.7	59.5	37.7	1.6	1.9	3.5	1.4	11.2	2.6
U	0.7	3.6	1.8	0.6	1.6	0.8	0.5	1.3	0.7	0.8	2.2	0.7	1	0.4	0.7	0.7	1.6	1.4	36.7	0.8	0.7	0.7	0.6	0.7	2.5

Appendix 2

Table 8.5. Determined concentrations, expanded uncertainty and normalized error test result for MACS-3 calibrated to NIST 612.

MACS-3			40 µm				65 µm				100 µm			
	x_{ref}, ppm	Rel. U_{ref}, %	x, ppm	U, ppm	Rel. U, %	E_n	x, ppm	U, ppm	Rel. U, %	E_n	x, ppm	U, ppm	Rel. U, %	E_n
Na	5900	13.6%	6240	1497	24.0%	0.20	5561	500.25	9.0%	0.36	5501	398.11	7.2%	0.45
P			N/A				150.0	47.84	31.9%		143.5	44.23	30.8%	
Ca	269370	2.8%	285912	68672	24.0%	0.24	257859	24297	9.4%	0.45	261296	14514	5.6%	0.50
Sc	21	7.6%	21.94	4.19	19.1%	0.21	22.86	2.34	10.2%	0.66	23.67	2.86	12.1%	0.82
Ti	54.9	0.7%	66.08	17.78	26.9%	0.63	60.84	10.61	17.4%	0.56	61.13	8.40	13.7%	0.74
V	46.3	4.9%	54.79	15.32	28.0%	0.55	46.69	9.17	19.6%	0.04	45.14	4.35	9.6%	0.24
Cr	117	8.5%	159.2	60.58	38.0%	0.69	132.7	51.23	38.6%	0.30	130.1	17.16	13.2%	0.66
Mn	536	10.4%	564.9	159.50	28.2%	0.17	513.7	76.81	15.0%	0.23	502.2	48.09	9.6%	0.46
Co	57.1	7.0%	57.67	14.03	24.3%	0.04	51.55	3.90	7.6%	0.99	51.77	4.32	8.3%	0.91
Ni	57.4	17.1%	61.25	48.53	79.2%	0.08	54.85	41.87	76.3%	0.06	53.93	6.67	12.4%	0.29
Cu	120	8.3%	116.8	38.29	32.8%	0.08	104.5	25.73	24.6%	0.56	100.6	43.81	43.5%	0.43
Zn	111	10.3%	127.9	29.09	22.7%	0.54	110.4	13.04	11.8%	0.03	111.0	11.74	10.6%	0.00
Ga	16.1	13.7%	20.25	5.01	24.8%	0.76	16.47	2.88	17.5%	0.10	16.09	2.04	12.7%	0.00
Rb			0.37	0.44	116.7%		0.08	0.05	61.8%		0.18	0.55	301.8%	
Sr	6760	10.4%	7461	1959.51	26.3%	0.34	6793	744.65	11.0%	0.03	6834	562.20	8.2%	0.08
Y	22.4	8.0%	22.20	4.51	20.3%	0.04	23.19	2.44	10.5%	0.26	24.44	2.35	9.6%	0.69
Zr	8.67	14.5%	9.29	2.08	22.4%	0.26	9.09	1.16	12.8%	0.25	9.67	0.75	7.8%	0.68
Nb	53.4	17.6%	56.88	17.83	31.3%	0.17	53.11	7.25	13.7%	0.02	54.74	4.49	8.2%	0.13
Mo	1.21	23.1%	1.69	0.73	43.0%	0.62	1.39	0.35	25.3%	0.41	1.36	0.20	15.1%	0.42
Ag	53.3	6.8%	80.28	24.91	31.0%	1.07	60.33	13.91	23.1%	0.49	58.43	7.47	12.8%	0.62
Cd	54.6	8.1%	62.15	15.84	25.5%	0.46	55.89	6.25	11.2%	0.17	56.81	4.78	8.4%	0.34
Sn	58.1	30.3%	65.18	18.46	28.3%	0.28	54.47	11.26	20.7%	0.17	53.18	3.16	5.9%	0.28
Sb	20.6	10.7%	34.18	11.39	33.3%	1.17	26.85	5.32	19.8%	1.09	25.85	2.80	10.8%	1.47
Cs			<LOD				0.05	0.08	174.8%		0.02	0.02	60.6%	
Ba	58.7	6.8%	63.08	14.38	22.8%	0.29	56.84	8.37	14.7%	0.20	55.57	3.91	7.0%	0.56
La	10.4	9.6%	11.41	2.21	19.4%	0.42	10.74	1.02	9.5%	0.24	11.22	0.76	6.8%	0.65
Ce	11.2	5.9%	12.37	3.36	27.2%	0.34	10.67	1.12	10.5%	0.41	10.78	0.75	7.0%	0.42
Pr	12.1	3.8%	12.51	3.13	25.1%	0.13	11.00	1.00	9.1%	1.00	11.32	0.97	8.6%	0.73
Nd	11	7.5%	11.29	2.65	23.5%	0.10	11.04	1.09	9.9%	0.03	11.25	0.80	7.1%	0.22
Sm	11	4.9%	10.86	1.73	16.0%	0.08	10.57	0.93	8.8%	0.40	11.03	0.86	7.8%	0.03
Eu	11.8	2.2%	11.75	2.42	20.6%	0.02	10.77	1.24	11.6%	0.81	11.14	0.64	5.7%	0.97
Gd	10.8	5.6%	10.23	2.21	21.6%	0.25	10.45	0.84	8.1%	0.34	11.04	1.00	9.1%	0.20
Tb	10.9	1.7%	10.18	1.94	19.1%	0.37	10.49	1.22	11.6%	0.33	10.89	0.80	7.3%	0.02
Dy	10.7	9.3%	11.18	2.37	21.2%	0.18	11.21	1.26	11.2%	0.32	11.77	0.91	7.7%	0.80
Ho	11.3	2.5%	11.23	2.40	21.3%	0.03	11.44	1.17	10.3%	0.11	11.99	1.04	8.7%	0.64
Er	11.2	3.9%	11.25	2.09	18.6%	0.02	11.46	1.25	10.9%	0.20	11.96	1.07	8.9%	0.66
Tm	11.9	4.4%	11.78	2.55	21.7%	0.04	12.06	1.16	9.6%	0.12	12.77	0.91	7.1%	0.83
Yb	11.6	3.4%	12.17	2.48	20.4%	0.23	12.12	1.32	10.9%	0.38	12.76	1.09	8.6%	0.99
Lu	10.8	5.6%	11.30	1.82	16.1%	0.26	11.68	1.38	11.8%	0.59	12.24	0.98	8.0%	1.26
Hf	4.73	8.9%	5.18	1.16	22.4%	0.37	5.08	0.65	12.7%	0.45	5.28	0.41	7.7%	0.95
Ta	20.5	51.7%	25.17	5.69	22.6%	0.39	24.12	3.42	14.2%	0.33	24.74	2.17	8.8%	0.39
Pb	56.5	6.4%	77.45	22.65	29.2%	0.91	61.58	9.35	15.2%	0.51	60.15	4.81	8.0%	0.61
Bi	19.9	16.1%	28.08	8.86	31.5%	0.87	20.94	5.49	26.2%	0.16	20.27	3.36	16.6%	0.08
Th	55.4	4.0%	55.47	10.26	18.5%	0.01	56.58	5.03	8.9%	0.22	58.88	4.21	7.1%	0.73
U	1.52	5.3%	1.67	0.69	41.2%	0.22	1.44	0.39	27.0%	0.21	1.43	0.24	17.1%	0.35

Table 8.6. Determined concentrations, expanded uncertainty and normalized error test result for CAL-S calibrated to MACS-3. For calibration of P, Rb and Cs NIST 612 was used.

CAL-S			40 µm				65 µm				100 µm			
	x_{ref}, ppm	Rel. U_{ref}, %	x, ppm	U, ppm	Rel. U, %	E_n	x, ppm	U, ppm	Rel. U, %	E_n	x, ppm	U, ppm	Rel. U, %	E_n
Na			118.5	70.38	59.4%		113.9	41.31	36.3%		113.9	40.90	35.9%	
P			<LOD				43.78				21.67			
Ca			377141	106410	28.2%		412826	55841	13.5%		396339	37993	9.6%	
Sc			<LOD				<LOD				0.11	0.05	49.3%	
Ti			4.37	3.30	75.4%		5.47	4.28	78.3%		5.77	4.52	78.4%	
V			1.19	0.60	50.6%		1.34	0.46	34.4%		1.38	0.20	14.3%	
Cr	3.395	13.3%	3.53	2.18	61.9%	0.06	3.51	1.59	45.2%	0.07	3.22	0.74	23.0%	0.21
Mn			9.64	3.57	37.1%		9.35	1.61	17.3%		9.19	1.33	14.4%	
Co	0.84	16.4%	0.43	1.24	286.3%	0.32	0.06	0.05	88.5%	5.31	0.05	0.03	56.6%	5.65
Ni			8.84	14.47	163.7%		3.69	3.61	97.7%		3.91	3.50	89.5%	
Cu			1.36	1.47	108.2%		1.13	0.93	81.8%		1.05	0.42	40.3%	
Zn	15	10.6%	11.50	7.98	69.4%	0.43	10.97	3.09	28.1%	1.16	11.98	2.83	23.6%	0.93
Ga			0.15	0.15	96.3%		0.05	0.04	85.5%		0.05	0.08	160.4%	
Rb			1.61				0.11				0.11			
Sr	233	7.0%	206.8	71.43	34.5%	0.36	221.2	35.41	16.0%	0.31	222.9	33.33	14.9%	0.28
Y	2.2	14.2%	1.85	0.42	22.6%	0.67	1.78	0.27	15.4%	1.00	1.74	0.23	13.5%	1.19
Zr			0.31	0.31	100.2%		0.30	0.18	62.1%		0.35	0.38	106.8%	
Nb			0.03	0.03	85.2%		0.03	0.02	71.3%		0.03	0.02	52.3%	
Mo	0.2	20.4%	0.15	0.15	103.3%	0.34	0.12	0.08	65.8%	0.98	0.12	0.05	42.4%	1.23
Ag			<LOD				0.21	0.17	81.1%		0.04	0.07	199.8%	
Cd	0.365	18.6%	0.43	0.50	115.5%	0.13	0.29	0.19	65.2%	0.37	0.27	0.09	32.3%	0.84
Sn			0.20	0.13	68.3%		0.15	0.31	204.5%		0.09	0.11	122.4%	
Sb			0.13	0.25	189.4%		0.05	0.04	70.6%		0.04	0.02	62.1%	
Cs	0.013	30.8%	<LOD				<LOD				<LOD			
Ba			1.63	0.88	53.6%		1.56	0.55	35.2%		1.71	0.64	37.3%	
La	0.89	16.2%	0.76	0.16	20.8%	0.60	0.77	0.14	17.8%	0.58	0.76	0.11	14.1%	0.74
Ce	0.4	18.5%	0.31	0.20	63.7%	0.41	0.35	0.29	82.2%	0.15	0.30	0.06	18.9%	1.02
Pr	0.1	22.6%	0.09	0.03	35.8%	0.31	0.10	0.04	35.9%	0.08	0.09	0.03	29.8%	0.16
Nd	0.391	18.4%	0.36	0.13	35.9%	0.23	0.38	0.13	34.6%	0.09	0.36	0.06	16.6%	0.33
Sm	0.071	23.8%	0.09	0.08	90.2%	0.18	0.07	0.03	43.3%	0.10	0.07	0.04	51.1%	0.04
Eu	0.02	29.0%	0.03	0.04	121.0%	0.27	0.02	0.01	66.3%	0.01	0.02	0.02	80.1%	0.06
Gd	0.101	22.6%	0.12	0.10	85.1%	0.20	0.10	0.04	40.7%	0.01	0.10	0.04	43.8%	0.07
Tb	0.017	29.4%	0.02	0.02	105.9%	0.14	0.02	0.01	35.8%	0.05	0.02	0.01	51.1%	0.07
Dy	0.1105	22.3%	0.11	0.09	87.5%	0.04	0.10	0.05	45.0%	0.17	0.10	0.02	24.0%	0.42
Ho	0.0286	27.3%	0.03	0.02	61.2%	0.21	0.03	0.01	37.8%	0.04	0.03	0.00	16.4%	0.11
Er	0.08772	23.1%	0.10	0.07	73.7%	0.15	0.08	0.03	38.1%	0.21	0.09	0.02	23.2%	0.01
Tm	0.012	31.7%	0.02	0.01	80.0%	0.24	0.01	0.01	58.9%	0.15	0.01	0.00	25.9%	0.03
Yb	0.07489	23.6%	0.09	0.09	95.8%	0.22	0.07	0.02	28.2%	0.25	0.07	0.02	25.5%	0.19
Lu	0.0107	31.8%	0.02	0.01	74.1%	0.49	0.01	0.01	49.0%	0.12	0.01	0.00	33.7%	0.35
Hf			0.01	0.01	131.3%		0.01	0.02	132.2%		0.01	0.01	105.3%	
Ta			0.00	0.01	164.4%		0.00	0.01	164.5%		0.00	0.01	154.0%	
Pb			1.15	0.86	75.2%		1.54	1.28	83.5%		1.25	1.02	81.5%	
Bi			0.01	0.06	460.7%		0.01	0.01	124.1%		0.01	0.01	130.3%	
Th			0.03	0.03	103.3%		0.03	0.02	64.9%		0.03	0.02	58.8%	
U	0.8162	16.5%	0.69	0.24	35.1%	0.47	0.76	0.15	19.8%	0.26	0.72	0.08	11.3%	0.60

Table 8.7. Determined concentrations, expanded uncertainty and normalized error test result for Es-14 calibrated to MACS-3. For calibration of P, Rb and Cs NIST 612 was used.

Es-14			40 µm				65 µm				100 µm			
	x_{ref}, ppm	Rel. U_{ref}, %	x, ppm	U, ppm	Rel. U, %	E_n	x, ppm	U, ppm	Rel. U, %	E_n	x, ppm	U, ppm	Rel. U, %	E_n
Na			265.3	84.16	31.7%		289.8	80.21	27.7%		298.9	90.49	30.3%	
P	91.6	48%	111.4	426.42	382.8%	0.05	114.0	69.32	60.8%	0.27	82.04	27.93	34.0%	0.19
Ca	324045	3%	344377	65160	18.9%	0.31	327465	32701	10.0%	0.10	324262	25089	7.7%	0.01
Sc	2.02	63%	2.10	0.81	38.8%	0.05	1.91	0.40	21.0%	0.09	2.06	0.34	16.4%	0.03
Ti	623	21%	601.5	574.75	95.5%	0.04	587.6	379.06	64.5%	0.09	644.2	784.58	121.8%	0.03
V	12.54	41%	13.02	3.55	27.3%	0.08	14.51	4.08	28.1%	0.30	12.33	2.09	17.0%	0.04
Cr	70.62	91%	35.40	107.07	302.5%	0.28	31.23	44.97	144.0%	0.50	17.59	10.77	61.2%	0.81
Mn	116	53%	123.0	59.72	48.6%	0.08	115.6	29.89	25.9%	0.01	116.3	24.26	20.9%	0.00
Co	5.29	66%	3.62	3.72	102.5%	0.33	3.38	1.72	50.9%	0.49	2.90	0.85	29.2%	0.67
Ni	13.12	43%	10.88	9.32	85.7%	0.21	14.14	20.97	148.4%	0.05	8.78	3.76	42.9%	0.64
Cu	17.2	58%	12.90	8.06	62.5%	0.34	21.57	44.59	206.7%	0.10	12.18	3.32	27.3%	0.48
Zn	31.68	48%	13.87	14.69	105.9%	0.84	14.67	7.62	51.9%	1.00	16.96	32.02	188.8%	0.42
Ga	2.93	85%	2.52	0.79	31.2%	0.16	2.98	0.72	24.3%	0.02	2.60	0.60	23.2%	0.13
Rb	15.91	28%	18.59	5.96	32.1%	0.36	16.70	2.17	13.0%	0.16	16.72	3.37	20.1%	0.15
Sr	494	21%	524.6	133.13	25.4%	0.18	519.5	88.29	17.0%	0.19	512.8	87.38	17.0%	0.14
Y	6.9	48%	6.67	2.05	30.7%	0.06	6.83	4.51	66.0%	0.01	6.64	1.91	28.8%	0.07
Zr	27.14	48%	13.82	9.33	67.5%	0.83	17.75	24.86	140.1%	0.33	17.85	24.72	138.4%	0.33
Nb	5.65	33%	2.96	2.89	97.5%	0.79	3.30	1.65	50.0%	0.95	4.00	5.13	128.5%	0.30
Mo	0.78	77%	0.75	0.58	77.3%	0.03	0.83	0.94	113.4%	0.05	0.67	0.39	59.1%	0.16
Ag	2.88	52%	1.81	2.55	140.9%	0.36	3.53	7.37	208.8%	0.09	2.42	3.52	145.3%	0.12
Cd	8.12	27%	8.59	23.94	278.6%	0.02	8.33	16.68	200.3%	0.01	5.30	2.03	38.4%	0.94
Sn	20.6	11%	21.78	28.44	130.6%	0.04	21.10	11.31	53.6%	0.04	20.45	18.80	91.9%	0.01
Sb	5.75	37%	5.18	3.14	60.5%	0.15	7.70	5.08	66.0%	0.35	9.95	17.99	180.8%	0.23
Cs	0.76	8%	1.06	1.14	107.2%	0.27	0.78	0.18	23.6%	0.12	0.74	0.15	19.8%	0.15
Ba	233	54%	113.7	71.94	63.3%	0.82	161.9	199.87	123.4%	0.30	148.9	108.99	73.2%	0.51
La	7.52	37%	6.27	1.71	27.3%	0.38	6.37	2.09	32.9%	0.33	5.88	1.00	17.1%	0.55
Ce	13.04	70%	11.39	3.04	26.6%	0.17	12.29	3.26	26.5%	0.08	10.93	1.72	15.7%	0.23
Pr	1.72	9%	2.42	5.58	230.2%	0.13	1.64	0.43	25.9%	0.18	1.59	0.20	12.7%	0.50
Nd	7.27	12%	7.04	5.17	73.4%	0.04	6.61	3.06	46.3%	0.21	6.28	1.62	25.8%	0.54
Sm	1.33	33%	1.24	0.69	55.8%	0.11	1.29	0.49	38.3%	0.06	1.25	0.14	11.3%	0.18
Eu	0.3	13%	0.29	0.07	25.1%	0.15	0.30	0.10	34.8%	0.01	0.27	0.03	9.2%	0.55
Gd	1.42	14%	1.23	0.42	33.9%	0.40	1.33	0.75	56.5%	0.12	1.22	0.25	20.1%	0.63
Tb	0.2	20%	0.19	0.09	47.3%	0.14	0.19	0.14	71.7%	0.08	0.18	0.03	16.9%	0.35
Dy	1.2	17%	1.08	0.34	31.4%	0.31	1.02	0.30	29.4%	0.49	1.04	0.24	23.3%	0.50
Ho	0.24	17%	0.22	0.09	41.9%	0.20	0.22	0.14	63.2%	0.11	0.22	0.05	25.0%	0.33
Er	0.65	15%	0.64	0.22	34.1%	0.04	0.64	0.69	108.4%	0.02	0.62	0.21	33.7%	0.13
Tm	0.093	11%	0.08	0.03	40.1%	0.49	0.09	0.06	67.0%	0.09	0.08	0.03	37.0%	0.25
Yb	0.55	7%	0.51	0.16	30.9%	0.24	0.56	0.40	71.0%	0.03	0.54	0.22	41.5%	0.05
Lu	0.08	25%	0.07	0.03	43.8%	0.16	0.08	0.05	66.0%	0.07	0.08	0.05	56.7%	0.04
Hf	0.6	13%	0.39	0.21	55.3%	0.94	0.64	1.08	169.2%	0.04	0.60	1.14	189.3%	0.00
Ta	0.14	29%	0.09	0.10	107.9%	0.41	0.12	0.09	82.0%	0.24	0.16	0.28	173.1%	0.07
Pb	126	21%	147.9	320.17	216.5%	0.07	152.5	131.18	86.0%	0.20	113.6	80.81	71.1%	0.14
Bi	34.67	25%	13.61	24.17	177.6%	0.82	19.39	27.22	140.4%	0.54	18.77	28.36	151.1%	0.54
Th	1.53	21%	2.03	4.10	202.3%	0.12	1.47	0.54	36.9%	0.10	1.50	0.40	26.9%	0.07
U	0.64	25%	0.64	0.34	53.4%	0.00	0.70	0.39	55.5%	0.15	0.66	0.20	29.9%	0.09

Table 8.8. Determined concentrations, expanded uncertainty and normalized error test result for Es-18 calibrated to MACS-3. For calibration of P, Rb and Cs NIST 612 was used.

Es-18			40 µm				65 µm				100 µm			
	x_{ref}, ppm	Rel. U_{ref}, %	x, ppm	U, ppm	Rel. U, %	E_n	x, ppm	U, ppm	Rel. U, %	E_n	x, ppm	U, ppm	Rel. U, %	E_n
Na			240.2	377.70	157.2%		223.3	78.34	35.1%		238.8	115.08	48.2%	
P	113	92%	1029	57294.52	5567.0%	0.02	193.5	130.46	67.4%	0.48	177.2	72.69	41.0%	0.50
Ca	206334	3%	204333	47352	23.2%	0.04	213151	23481	11.0%	0.28	203036	15602	7.7%	0.20
Sc	1.14		1.24	0.63	50.5%		1.53	1.51	99.0%		1.40	0.47	33.8%	
Ti	372	29%	272.9	288.39	105.7%	0.32	393.2	609.75	155.1%	0.03	349.8	259.73	74.2%	0.08
V	20.8	59%	18.39	4.54	24.7%	0.18	20.31	3.09	15.2%	0.04	19.05	2.45	12.9%	0.14
Cr	10.67	103%	7.60	3.23	42.5%	0.27	9.73	1.97	20.2%	0.08	15.26	48.93	320.5%	0.09
Mn	410	15%	446.6	168.10	37.6%	0.20	436.3	81.16	18.6%	0.25	437.4	75.05	17.2%	0.28
Co			0.81	0.36	43.7%		0.87	0.33	38.4%		0.83	0.19	23.3%	
Ni			1.91	0.82	42.8%		2.52	1.32	52.2%		2.40	1.42	59.2%	
Cu	1.95	88%	0.92	0.77	83.5%	0.55	0.79	0.65	82.1%	0.63	0.98	1.08	110.1%	0.48
Zn	7.94	104%	7.45	3.96	53.2%	0.05	6.83	1.55	22.7%	0.13	6.71	1.63	24.3%	0.15
Ga	1.81	63%	1.41	0.85	60.4%	0.28	1.54	0.46	29.5%	0.22	1.62	0.65	40.2%	0.15
Rb	8.92	37%	12.98	10.92	84.1%	0.36	11.26	2.96	26.2%	0.53	12.82	7.63	59.5%	0.47
Sr	51.43	6%	48.56	13.40	27.6%	0.21	50.04	8.22	16.4%	0.16	49.70	8.34	16.8%	0.20
Y	7.24	18%	5.22	1.94	37.2%	0.86	6.22	5.44	87.5%	0.18	6.34	3.80	59.9%	0.22
Zr	31.27	15%	9.81	6.71	68.4%	2.61	12.36	9.83	79.5%	1.73	17.30	44.36	256.4%	0.31
Nb	1.99	113%	0.83	0.54	65.0%	0.51	1.17	0.58	49.3%	0.36	1.08	0.69	64.0%	0.39
Mo			0.06	0.07	116.6%		0.06	0.14	229.6%		0.04	0.03	60.8%	
Ag	<0.5		<LOD				<LOD				<LOD			
Cd	0.065	145%	<LOD				<LOD				0.08	0.05	69.6%	0.09
Sn	0.14		0.29	0.26	90.1%		0.26	0.16	58.9%		0.25	0.11	42.2%	
Sb			<LOD				0.04	0.02	66.3%		0.04	0.06	140.1%	
Cs	0.41	24%	0.50	0.33	65.6%	0.26	0.47	0.09	18.8%	0.42	0.49	0.12	24.3%	0.49
Ba	31.92	9%	29.72	60.14	202.3%	0.04	32.20	43.62	135.5%	0.01	37.03	43.19	116.6%	0.12
La	6.34	17%	6.22	5.24	84.2%	0.02	6.62	8.55	129.2%	0.03	9.91	25.81	260.3%	0.14
Ce	10.8	13%	12.81	8.25	64.4%	0.24	13.29	16.11	121.2%	0.15	12.85	7.54	58.7%	0.27
Pr	1.43	7%	1.57	1.42	90.4%	0.10	1.45	0.42	29.1%	0.04	1.59	0.69	43.4%	0.23
Nd	6.82	36%	5.63	5.35	95.1%	0.20	5.99	5.63	94.0%	0.14	6.23	4.44	71.2%	0.12
Sm	1.23	8%	1.26	1.05	83.4%	0.03	1.31	0.92	70.4%	0.08	1.16	0.41	35.6%	0.16
Eu	0.27	7%	0.33	0.42	129.7%	0.13	0.31	0.14	45.3%	0.26	0.37	0.56	150.4%	0.18
Gd	1.36	19%	1.22	0.62	51.2%	0.21	1.20	0.47	39.1%	0.30	1.64	2.93	179.3%	0.09
Tb	0.19	11%	0.17	0.07	42.4%	0.22	0.17	0.07	41.5%	0.23	0.17	0.03	15.7%	0.58
Dy	1.24	6%	0.90	0.30	33.8%	1.08	0.98	0.57	57.9%	0.45	0.94	0.21	22.4%	1.31
Ho	0.22	9%	0.17	0.04	22.4%	1.04	0.21	0.19	90.2%	0.07	0.21	0.16	73.9%	0.06
Er	0.61	20%	0.46	0.10	21.1%	0.94	0.51	0.17	32.6%	0.50	0.55	0.26	46.9%	0.20
Tm	0.077	16%	0.07	0.04	53.3%	0.27	0.09	0.15	164.0%	0.10	0.08	0.08	91.2%	0.09
Yb	0.54	11%	0.35	0.20	57.2%	0.90	0.42	0.11	26.2%	0.93	0.48	0.28	57.3%	0.20
Lu	0.074	11%	0.05	0.03	53.1%	0.65	0.10	0.30	281.8%	0.10	0.07	0.07	98.4%	0.09
Hf	0.85	28%	0.35	0.39	111.1%	1.10	0.41	0.48	115.7%	0.82	0.35	0.26	74.4%	1.40
Ta	0.1	40%	0.06	0.06	101.2%	0.51	0.07	0.05	74.0%	0.48	0.07	0.05	79.3%	0.48
Pb			0.93	1.07	116.2%		0.71	0.43	60.3%		1.12	1.97	176.1%	
Bi	<1		0.03	0.03	121.3%		0.02	0.04	140.8%		0.02	0.03	118.9%	
Th	1.23	8%	1.15	0.42	36.8%	0.18	1.50	2.00	133.1%	0.14	1.25	0.39	31.5%	0.04
U			0.44	0.28	64.5%		0.58	0.48	83.9%		0.60	0.45	76.1%	

Table 8.9. Determined concentrations, expanded uncertainty and normalized error test result for Es-17 calibrated to MACS-3. For calibration of P, Rb and Cs NIST 612 was used.

Es-17			40 µm				65 µm				100 µm			
	x_{ref}, ppm	Rel. U_{ref}, %	x, ppm	U, ppm	Rel. U, %	E_n	x, ppm	U, ppm	Rel. U, %	E_n	x, ppm	U, ppm	Rel. U, %	E_n
Na	319	120.9%	202.8	93.77	46.2%	0.29	205.7	119.48	58.1%	0.28	190.9	43.30	22.7%	0.33
P	65.46	93.3%	<LOD				31.01	14.99	48.3%	0.55	32.93	18.15	55.1%	0.51
Ca	291526	3.2%	300401	51462	17.1%	0.17	305208	29459	9.7%	0.44	290756	23525	8.1%	0.03
Sc	2.18		2.05	0.58	28.2%		1.82	0.30	16.5%		1.66	0.25	15.2%	
Ti	534	22.5%	451.6	109.68	24.3%	0.50	520.4	200.35	38.5%	0.06	549.0	193.17	35.2%	0.07
V	9.6	53.1%	8.63	2.78	32.2%	0.17	8.88	1.12	12.6%	0.14	9.35	0.98	10.5%	0.05
Cr	7.28	74.2%	7.49	2.61	34.8%	0.04	7.57	1.55	20.5%	0.05	8.21	1.44	17.5%	0.17
Mn	232	20.0%	219.2	67.43	30.8%	0.16	226.9	65.01	28.7%	0.07	225.8	48.25	21.4%	0.10
Co	0.98	120.4%	1.53	0.74	48.5%	0.40	1.50	0.19	13.0%	0.43	1.39	0.23	16.7%	0.34
Ni	5.37	118.1%	3.81	2.55	66.8%	0.23	3.96	1.16	29.3%	0.22	4.13	1.49	36.0%	0.19
Cu	3.64	97.8%	2.21	3.24	146.6%	0.30	2.14	0.92	43.1%	0.41	2.36	2.03	86.0%	0.31
Zn	8.88	52.0%	7.92	3.81	48.1%	0.16	8.83	2.02	22.8%	0.01	8.54	1.99	23.3%	0.07
Ga	3.02	73.5%	2.21	0.90	40.6%	0.34	2.49	0.56	22.5%	0.23	2.57	0.47	18.2%	0.20
Rb	15.16	21.9%	18.81	4.90	26.1%	0.62	16.91	3.94	23.3%	0.34	15.13	1.75	11.5%	0.01
Sr	137	11.0%	110.5	23.62	21.4%	0.96	132.2	23.54	17.8%	0.18	131.9	24.15	18.3%	0.19
Y	8.91	13.5%	8.05	1.60	19.9%	0.43	9.09	7.45	81.9%	0.02	7.13	0.94	13.3%	1.17
Zr	23.98	26.8%	10.48	4.19	40.0%	1.76	13.45	8.38	62.3%	1.00	13.08	6.80	52.0%	1.17
Nb	2.19	58.4%	1.63	1.01	61.8%	0.34	1.88	0.95	50.8%	0.20	1.74	0.44	25.3%	0.34
Mo	0.57	42.1%	0.61	2.20	359.4%	0.02	0.54	0.57	106.9%	0.06	0.91	1.91	210.1%	0.18
Ag	<0.5		<LOD				<LOD				<LOD			
Cd	0.011	109.1%	<LOD				<LOD				0.05	0.05	94.2%	0.82
Sn	0.25		0.31	0.29	92.8%		0.32	0.14	42.8%		0.33	0.13	38.9%	
Sb	0.26	123.1%	0.08	0.06	75.1%	0.56	0.05	0.04	76.0%	0.64	0.10	0.25	253.0%	0.40
Cs	0.51	11.8%	0.69	0.24	34.4%	0.73	0.63	0.24	37.9%	0.48	0.54	0.09	16.2%	0.28
Ba	46.88	34.9%	45.05	24.03	53.3%	0.06	50.26	37.61	74.8%	0.08	42.92	16.63	38.7%	0.17
La	15.12	29.9%	13.39	3.67	27.4%	0.30	13.22	2.32	17.5%	0.37	12.43	2.02	16.2%	0.54
Ce	22.37	19.3%	29.12	28.80	98.9%	0.23	29.93	8.39	28.0%	0.80	30.91	11.02	35.7%	0.72
Pr	2.78	7.2%	2.71	0.61	22.4%	0.11	2.92	0.58	19.8%	0.23	2.77	0.39	13.9%	0.03
Nd	11.53	26.5%	10.70	2.38	22.2%	0.22	10.06	1.56	15.5%	0.43	9.25	1.24	13.4%	0.69
Sm	1.83	6.6%	1.79	0.51	28.7%	0.08	1.85	0.32	17.2%	0.05	1.70	0.25	14.8%	0.48
Eu	0.39	15.4%	0.40	0.09	22.8%	0.06	0.43	0.10	22.9%	0.33	0.38	0.06	15.0%	0.18
Gd	1.97	10.2%	2.79	1.88	67.6%	0.43	3.57	2.87	80.4%	0.56	2.53	2.11	83.4%	0.26
Tb	0.24	8.3%	0.25	0.05	20.3%	0.17	0.25	0.17	65.7%	0.09	0.22	0.03	15.2%	0.63
Dy	1.48	8.1%	1.18	0.23	19.4%	1.18	1.46	1.43	97.5%	0.01	1.12	0.20	17.9%	1.52
Ho	0.26	7.7%	0.22	0.08	36.6%	0.43	0.29	0.26	91.9%	0.10	0.23	0.03	14.3%	0.90
Er	0.69	5.8%	0.62	0.18	29.6%	0.40	0.72	0.60	83.8%	0.04	0.58	0.08	14.5%	1.24
Tm	0.081	7.4%	0.08	0.04	46.3%	0.05	0.10	0.09	90.8%	0.18	0.08	0.01	17.5%	0.14
Yb	0.56	7.1%	0.49	0.09	18.5%	0.69	0.51	0.06	12.4%	0.73	0.49	0.12	24.6%	0.55
Lu	0.08		0.07	0.02	25.3%		0.08	0.05	59.5%		0.07	0.02	28.3%	
Hf	0.59	13.6%	0.40	0.16	38.9%	1.08	0.47	0.23	48.3%	0.48	0.47	0.20	41.3%	0.55
Ta	0.08	85.0%	0.11	0.08	73.8%	0.31	0.13	0.09	70.3%	0.45	0.15	0.14	96.1%	0.43
Pb	3.54	23.2%	4.06	7.67	188.7%	0.07	3.95	2.24	56.6%	0.17	3.97	1.97	49.7%	0.20
Bi	<1		<LOD				0.03	0.02	71.7%		0.02	0.01	46.4%	
Th	2.96	33.1%	3.27	0.64	19.5%	0.26	3.38	0.40	11.9%	0.40	3.09	0.38	12.4%	0.13
U			0.67	0.27	40.9%		0.69	0.11	15.2%		0.71	0.10	14.5%	

Table 8.10. Determined concentrations, expanded uncertainty and normalized error test result for Es-3 calibrated to MACS-3. For calibration of P, Rb and Cs NIST 612 was used.

Es-3			40 µm				65 µm				100 µm			
	x_{ref}, ppm	Rel. U_{ref}, %	x, ppm	U, ppm	Rel. U, %	E_n	x, ppm	U, ppm	Rel. U, %	E_n	x, ppm	U, ppm	Rel. U, %	E_n
Na			709.5	922.65	130.0%		436.7	182.57	41.8%		533.6	492.83	92.4%	
P	1850	10.8%	2508	4565.83	182.0%	0.14	2886	1848.17	64.0%	0.56	3307	1506.62	45.6%	0.96
Ca	362567	2.4%	364665	59164	16.2%	0.04	376855	37087	9.8%	0.37	366092	30295	8.3%	0.11
Sc	1.51	87.8%	2.51	1.04	41.5%	0.59	2.43	0.57	23.3%	0.64	2.30	0.31	13.3%	0.58
Ti	450	18.7%	388.0	284.46	73.3%	0.21	540.1	683.39	126.5%	0.13	532.4	126.58	23.8%	0.55
V	9.16	52.7%	7.12	2.51	35.3%	0.38	8.86	2.02	22.7%	0.06	9.69	1.83	18.9%	0.10
Cr	10.7	87.7%	7.80	3.19	40.9%	0.29	8.69	1.86	21.3%	0.21	9.66	1.87	19.4%	0.11
Mn	432	24.1%	481.1	279.89	58.2%	0.16	446.4	82.70	18.5%	0.11	528.4	145.38	27.5%	0.54
Co	2.05	8.8%	1.20	0.46	38.3%	1.71	1.22	0.44	36.5%	1.74	1.23	0.70	56.8%	1.14
Ni	3.61	96.5%	3.43	1.92	55.9%	0.05	5.28	5.50	104.2%	0.26	4.64	1.26	27.2%	0.28
Cu	4.25	28.7%	2.83	4.07	143.8%	0.33	1.92	0.67	34.8%	1.67	2.24	0.76	34.0%	1.40
Zn	5.81	78.3%	5.36	3.49	65.0%	0.08	5.66	2.69	47.5%	0.03	6.53	3.17	48.6%	0.13
Ga	2.26	74.6%	1.62	0.63	38.8%	0.36	1.94	0.45	23.3%	0.18	2.01	0.48	23.7%	0.14
Rb	9.06	45.2%	13.71	4.52	32.9%	0.76	13.74	2.61	19.0%	0.96	13.17	2.53	19.2%	0.86
Sr	187	18.2%	202.4	167.65	82.8%	0.09	178.7	33.94	19.0%	0.17	191.8	33.62	17.5%	0.10
Y	11.55	33.0%	15.96	10.63	66.6%	0.39	15.57	8.71	56.0%	0.42	15.01	3.70	24.6%	0.65
Zr	16.49	29.5%	9.75	5.20	53.3%	0.95	11.81	4.55	38.5%	0.70	14.05	11.06	78.8%	0.20
Nb	1.66	58.9%	5.76	5.71	99.0%	0.71	3.73	2.76	74.1%	0.71	5.50	5.98	108.7%	0.63
Mo	<1		0.24	0.21	87.7%		0.20	0.19	95.0%		0.25	0.21	83.3%	
Ag			<LOD				<LOD				0.07	0.08	108.6%	
Cd	0.17		<LOD				0.16	0.12	73.4%		0.14	0.16	117.5%	
Sn	<1		0.52	0.37	70.9%		0.43	0.24	56.3%		0.46	0.36	77.6%	
Sb	<0.1		0.19	0.15	80.9%		0.16	0.23	144.8%		0.16	0.12	74.3%	
Cs	0.56	32.5%	1.03	0.48	46.4%	0.92	0.88	0.24	27.4%	1.05	0.83	0.17	20.5%	1.09
Ba	39	96.4%	45.39	61.10	134.6%	0.09	37.11	9.90	26.7%	0.05	39.30	27.20	69.2%	0.01
La	8.31	15.5%	9.04	2.22	24.6%	0.28	9.67	1.85	19.2%	0.60	10.04	2.55	25.4%	0.61
Ce	13.31	51.8%	22.69	17.56	77.4%	0.50	23.34	14.02	60.1%	0.64	25.64	14.39	56.1%	0.77
Pr	2.05	5.9%	2.57	0.64	24.9%	0.80	2.62	0.46	17.5%	1.20	2.72	0.66	24.3%	1.00
Nd	8.37	30.7%	10.06	2.76	27.4%	0.45	10.36	2.00	19.4%	0.61	10.67	2.72	25.5%	0.61
Sm	1.93	13.9%	2.63	0.86	32.9%	0.77	2.51	0.50	19.8%	1.03	2.52	0.56	22.3%	0.95
Eu	0.42	12.9%	0.78	0.19	24.0%	1.85	0.66	0.20	30.7%	1.15	0.61	0.22	36.4%	0.84
Gd	2.07	14.0%	5.48	3.18	58.0%	1.07	5.03	3.02	60.0%	0.98	4.26	3.80	89.2%	0.57
Tb	0.3	15.3%	0.66	0.36	54.0%	1.00	0.52	0.13	25.9%	1.54	0.46	0.11	22.9%	1.40
Dy	1.73	15.5%	2.54	1.18	46.5%	0.67	2.36	0.68	29.1%	0.85	2.20	0.50	22.6%	0.84
Ho	0.35	15.4%	0.78	0.29	37.0%	1.46	0.62	0.15	24.6%	1.66	0.50	0.09	17.4%	1.45
Er	0.92	10.7%	1.42	0.70	49.6%	0.70	1.34	0.43	32.0%	0.95	1.21	0.20	16.2%	1.34
Tm	0.12	13.3%	0.39	0.26	66.0%	1.05	0.30	0.10	32.4%	1.82	0.25	0.08	31.7%	1.59
Yb	0.78	26.9%	1.13	0.46	40.9%	0.69	1.10	0.32	29.3%	0.84	0.98	0.25	25.5%	0.61
Lu	0.1	38.0%	0.32	0.16	49.1%	1.36	0.23	0.06	27.3%	1.79	0.20	0.06	29.0%	1.48
Hf	0.43	12.1%	0.47	0.15	31.9%	0.28	0.45	0.21	46.7%	0.08	0.47	0.19	40.0%	0.21
Ta	0.09	102.2%	0.37	0.46	123.9%	0.60	0.25	0.22	88.7%	0.67	0.18	0.14	81.5%	0.51
Pb	4.24	102.2%	3.61	3.31	91.6%	0.12	4.12	4.62	112.1%	0.02	4.41	3.07	69.7%	0.03
Bi	<0.5		0.16	0.29	185.6%		0.09	0.07	79.4%		0.08	0.03	43.8%	
Th	2	22.2%	3.21	0.63	19.6%	1.57	3.05	1.04	34.1%	0.93	2.72	0.48	17.7%	1.09
U	2.42	43.7%	2.56	1.25	48.8%	0.09	3.00	0.56	18.6%	0.49	3.39	1.08	31.9%	0.64

Table 8.11. Determined concentrations, expanded uncertainty and normalized error test result for Es-16 calibrated to MACS-3. For calibration of P, Rb and Cs NIST 612 was used.

Es-16			40 µm				65 µm				100 µm			
	x_{ref}, ppm	Rel. U_{ref}, %	x, ppm	U, ppm	Rel. U, %	E_n	x, ppm	U, ppm	Rel. U, %	E_n	x, ppm	U, ppm	Rel. U, %	E_n
Na	304	137%	1510	9364	620.2%	0.13	191.4	154.81	80.9%	0.25	173.0	38.12	22.0%	0.31
P	1012	14%	1403	5957.72	424.7%	0.07	1413	464.26	32.9%	0.83	1416	379.67	26.8%	1.00
Ca	220628	3%	210365	36981	17.6%	0.27	227716	20396	9.0%	0.33	220639	18501	8.4%	0.00
Sc	2.02		2.44	1.24	50.6%		2.32	0.38	16.3%		2.23	0.27	11.9%	
Ti	504	24%	335.9	93.56	27.9%	1.10	448.5	274.60	61.2%	0.18	448.9	251.13	55.9%	0.20
V	14	68%	7.69	2.62	34.1%	0.64	8.22	1.02	12.4%	0.60	8.27	1.22	14.7%	0.59
Cr	9.68	127%	8.14	3.25	39.9%	0.12	8.79	2.58	29.3%	0.07	10.91	9.39	86.0%	0.08
Mn	2091	7%	2099	463.71	22.1%	0.02	2282	385.77	16.9%	0.47	2186	341.74	15.6%	0.26
Co			0.98	0.55	55.6%		1.08	0.32	30.2%		0.90	0.22	24.7%	
Ni			2.46	1.85	75.2%		2.97	0.99	33.3%		2.73	1.07	39.2%	
Cu	3.95	106%	1.48	1.95	132.0%	0.54	1.97	2.66	135.1%	0.40	1.74	0.77	44.4%	0.52
Zn	14.88	107%	7.26	2.67	36.8%	0.47	8.27	2.80	33.9%	0.41	12.06	26.78	222.1%	0.09
Ga	1.82	32%	1.55	0.59	37.7%	0.33	1.77	0.37	21.2%	0.08	1.71	0.33	19.3%	0.16
Rb	10.53	37%	13.69	3.22	23.5%	0.63	13.62	3.28	24.1%	0.61	12.24	1.54	12.5%	0.41
Sr	59.64	6%	74.22	90.38	121.8%	0.16	60.64	9.54	15.7%	0.10	58.36	8.28	14.2%	0.14
Y	13.15	20%	12.78	3.34	26.1%	0.09	13.10	2.30	17.5%	0.01	12.56	1.96	15.6%	0.18
Zr	17.87	17%	8.05	3.97	49.3%	1.97	9.66	4.56	47.1%	1.50	10.63	7.85	73.8%	0.86
Nb	1.76	94%	0.96	0.49	50.8%	0.46	1.14	0.63	55.2%	0.35	1.23	0.66	53.4%	0.30
Mo	0.41	132%	0.13	0.22	164.9%	0.48	0.06	0.03	60.5%	0.65	0.06	0.03	46.9%	0.65
Ag	<0.5		<LOD				<LOD				<LOD			
Cd	0.043	79%	<LOD				0.10	0.09	92.0%	0.59	0.04	0.09	227.9%	0.06
Sn	0.13		0.36	0.34	95.7%		0.36	0.17	47.4%		0.34	0.18	53.2%	
Sb	0.27	119%	0.09	0.08	86.4%	0.54	0.06	0.03	45.9%	0.64	0.06	0.02	34.9%	0.65
Cs	0.62	13%	0.78	0.32	41.0%	0.50	0.75	0.16	21.0%	0.72	0.66	0.13	19.9%	0.24
Ba	41.58	72%	26.99	13.43	49.7%	0.45	30.84	8.81	28.6%	0.35	30.52	8.73	28.6%	0.36
La	10.6	17%	9.49	2.21	23.3%	0.38	9.93	1.92	19.3%	0.25	9.30	1.37	14.8%	0.57
Ce	14.93	24%	25.64	28.77	112.2%	0.37	23.52	16.43	69.9%	0.51	23.83	14.47	60.7%	0.60
Pr	2.31	15%	2.34	0.62	26.7%	0.04	2.64	0.54	20.3%	0.53	2.47	0.32	12.8%	0.34
Nd	11.33	36%	10.29	3.28	31.9%	0.20	10.66	2.39	22.4%	0.14	10.24	1.40	13.7%	0.25
Sm	2.29	13%	2.49	0.77	31.1%	0.24	2.50	0.59	23.6%	0.32	2.37	0.45	19.0%	0.15
Eu	0.52	12%	0.58	0.26	45.2%	0.21	0.57	0.13	22.8%	0.33	0.55	0.09	16.9%	0.30
Gd	2.67	4%	3.54	1.91	53.9%	0.46	3.73	2.28	61.1%	0.47	3.70	1.69	45.7%	0.61
Tb	0.36	6%	0.39	0.10	26.2%	0.33	0.37	0.09	24.3%	0.13	0.37	0.06	16.3%	0.12
Dy	2.29	6%	2.02	0.74	36.8%	0.36	2.11	0.35	16.4%	0.47	2.04	0.33	16.1%	0.70
Ho	0.4	10%	0.42	0.10	25.0%	0.16	0.41	0.07	16.5%	0.15	0.40	0.05	11.3%	0.01
Er	1.06	11%	1.09	0.14	12.8%	0.16	1.06	0.19	18.4%	0.02	1.03	0.14	13.2%	0.16
Tm	0.13	31%	0.15	0.05	32.5%	0.24	0.15	0.03	20.1%	0.34	0.14	0.02	14.3%	0.18
Yb	0.91	9%	0.88	0.29	33.0%	0.10	0.86	0.12	13.5%	0.38	0.86	0.08	9.8%	0.43
Lu	0.13	15%	0.13	0.04	33.1%	0.08	0.12	0.02	20.1%	0.36	0.12	0.01	10.9%	0.54
Hf	0.56	43%	0.24	0.10	40.7%	1.23	0.29	0.08	28.4%	1.08	0.34	0.20	58.7%	0.71
Ta	0.12	33%	0.07	0.07	94.3%	0.65	0.07	0.05	74.1%	0.68	0.09	0.09	99.7%	0.32
Pb			1.83	3.66	200.3%		1.99	1.50	75.2%		1.39	0.53	38.0%	
Bi	<1		0.03	0.05	165.9%		0.02	0.02	93.8%		0.02	0.01	46.8%	
Th	2.31	29%	2.40	0.94	39.2%	0.08	2.48	0.93	37.3%	0.15	2.31	0.41	17.7%	0.01
U			1.63	0.66	40.2%		1.96	0.54	27.4%		1.91	0.62	32.6%	

Non-exclusive licence to reproduce thesis and make thesis public

I, Martinš Jansons

1. herewith grant the University of Tartu a free permit (non-exclusive licence) to:

1.1. reproduce, for the purpose of preservation and making available to the public, including for addition to the *DSpace* digital archives until expiry of the term of validity of the copyright, and

1.2. make available to the public via the university's web environment, including via the DSpace digital archives, as of 30.05.2017 until expiry of the term of validity of the copyright,

“Characterization of natural sedimentary dolomite and limestone reference materials from Geological Survey of Estonia using LA-ICP-MS”

supervised by Kalle Kirsimäe and Päärn Paiste.

2. I am aware of the fact that the author retains these rights.

3. I certify that granting the non-exclusive licence does not infringe the intellectual property rights or rights arising from the Personal Data Protection Act.

Tartu, **27.05.2016**